ATOMIC ENERGY OF CANADA LIMITED

CHALK RIVER PROJECT

RESEARCH AND DEVELOPMENT

NRX ROD NO. 683

ANALYSIS OF IRRADIATED URANIUM AND ESTIMATION OF EFFECTIVE CROSS-SECTIONS

CRR-622 (REV)

BY

D.G. HURST, A.H. BOOTH, M. LOUNSBURY AND G.C. HANNA

CHALK RIVER, ONTARIO

JANUARY, 1956

REISSUED IN REVISED FORM

MAY, 1957

AECL NO. 447

ATOMIC ENERGY OF CANADA LIMITED
Chalk River Project
Research and Development

NRX ROD NO. 683

Analysis of Irradiated Uranium and Estimates of Effective Cross-Sections

CRR-622(Rev.)

Contents

Note: These papers were presented as CRR-622 at the Tripartite Reactor Core Conference at Chalk River, Ontario, January 9-12, 1956. They were revised in the summer of 1956 and issued in the Proceedings of the Conference (CRR-644-5). The present issue has been prepared directly from the Proceedings to permit a wider distribution.

Chalk River, Ontario
May 1957

NRX Rod 683: Part I

OUTLINE OF PROGRAM AND PREPARATION OF SPECIMENS

by
D. G. Hurst

The group of papers under this item covers measurements which have been made on material from NRX rod No. 683, one of the rods originally installed in the reactor. By September 1951 it had generated slightly more than 100 MWD energy, corresponding to a specific output from the central region of about 3100 MWD/Tonne. It was then removed from the reactor and held in storage as the principal item in an investigation of long irradiation. The intention was to study with material from the same specimen the various results of irradiation such as the distribution of plutonium isotopes in the rod, depletion of U-235, measurement of the changes in reactivity of material from several irradiation levels, and metallurgical effects. The present paper describes the general preparation for the work. Other papers will describe the details of the measurements. Chalk River reports on this work are listed as references 1, 2, 3, 4, and 5.

A joint program was arranged with USAEC, and the reactivity tests have been made in CP-2 at Argonne National Laboratory. Similar tests will be made at other facilities.

History of Rod 683.

The irradiation history of this rod is as follows:

(i) Originally installed in reactor at position F-26, 105.3 cm. from centre.

(ii) 18th January 1951, transferred to position D-12, 79.3 cm. from centre.

(iii) 24th September 1951, transferred to position F-16, 45.8 cm. from centre, for reactivity tests at "zero" power.

(iv) 30th September 1951, removed to storage.

Energy output = 68.0 MWD at F-26 plus 32.8 MWD at D-12

= 100.8 MWD total.

The energy output was calculated as the product of the integrated power and an output fraction assigned to the rod position. The output fraction is based on a flux distribution measured when the reactor was first put into operation. No account is taken of fine structure due to non-uniformities such as shutoff rod positions etc. Since values of nvt from this total energy output may have large errors it is likely that the values of nvt used finally will be based on measurements of depletion or other nuclear quantities.

Cutting Plan.

The program called for the rod to be cut into a number of specimens as shown in Figure 5.3.1. The cutting was done by the Operations Division and was carried out under water with an abrasive saw. The seven slugs, 12-1/4 inches long, are for reactivity measurements; the 1/8 inch lengths marked "chem" are discs from which U-235 depletion, Pu production, etc. averaged over the rod may be found; the 1/8 inch lengths marked "radial" were first removed as discs which were then cut transversely as shown in Figure 5.3.2 to provide the diametrical bars for determination of radial distributions. The segments left after removal of the bars have been put to various uses.

Measurements.

Before the rod was cut its length was measured and the outside diameter of the sheath was gauged every four inches along the length. The rod had shrunk 4-15/64 inches and had become slightly barrel-shaped with a maximum increase of 0.06 inch on the diameter at about 44 inches from the lower end.

The variation of gamma ray intensity along the length was measured with a specially constructed scintillation probe. Figure 5.3.3.

After cutting, the seven slugs for swing measurements, a 1/8 inch disc, and two 3-inch pieces for metallurgy were shipped to ANL.

The bars selected for the study of radial distribution were mounted in a lathe so that thin layers could be turned off to provide material from accurately known depths inside the rod. The turnings from chosen depths were dissolved and separated into

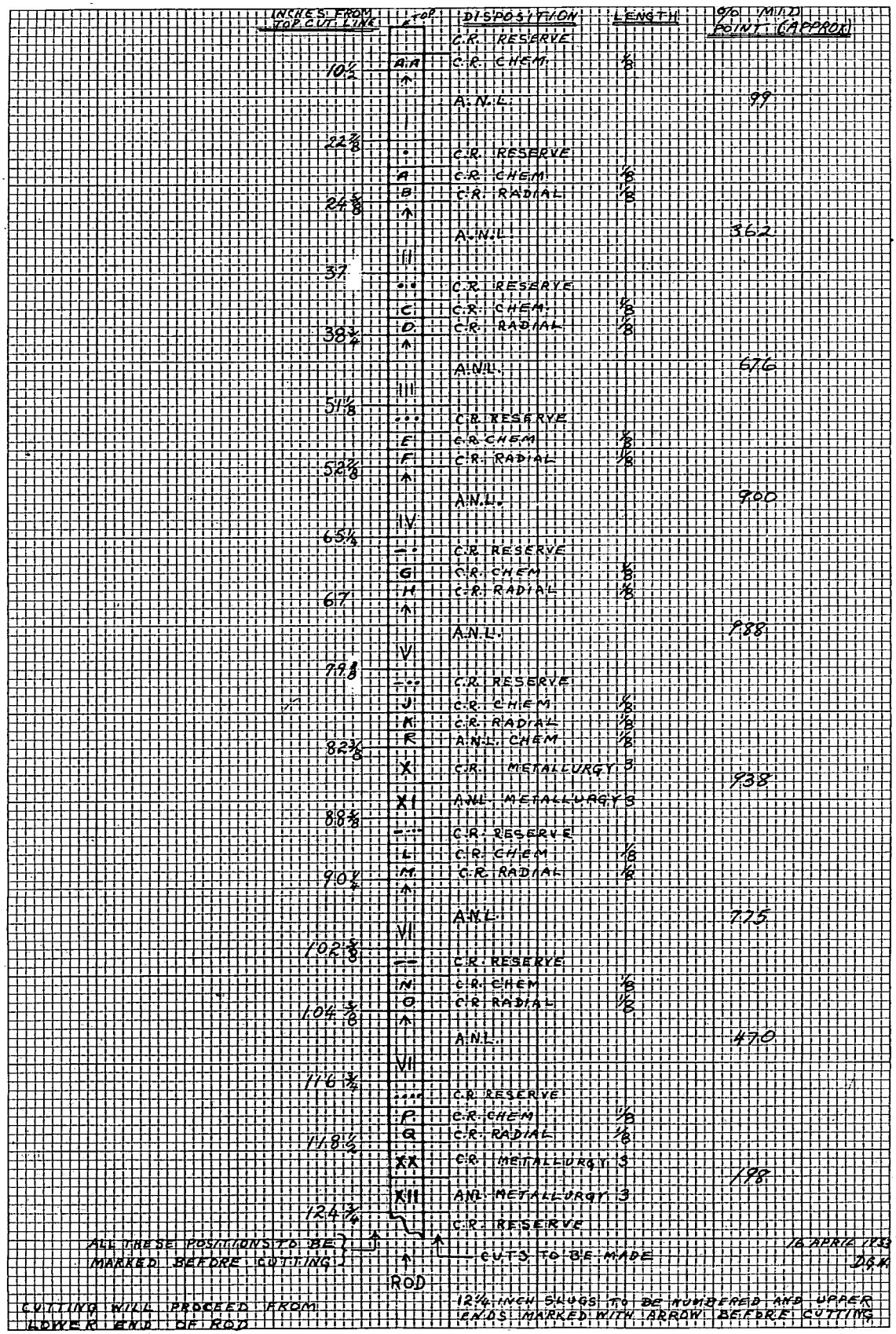
INCHES FROM TOP CUT LINE
TOP
DISPOSITION
LENGTH
% MILD POINT (APPROX)
C.R. RESERVE
C.R. CHEM.
1/8
10½
A
A.N.L.
99
22⅞
C.R. RESERVE
A
C.R. CHEM.
1/8
B
C.R. RADIAL
1/8
24⅜
A.N.L.
362
37
C.R. RESERVE
C
C.R. CHEM.
1/8
D
C.R. RADIAL
1/8
38¾
A.N.L.
676
51⅛
C.R. RESERVE
E
C.R. CHEM.
1/8
F
C.R. RADIAL
1/8
52⅜
A.N.L.
900
65¼
C.R. RESERVE
G
C.R. CHEM.
1/8
H
C.R. RADIAL
1/8
67
A.N.L.
988
79⅜
C.R. RESERVE
J
C.R. CHEM.
1/8
K
C.R. RADIAL
1/8
R
A.N.L. CHEM
1/8
82⅜
X
C.R. METALLURGY 3
938
XI
ANL METALLURGY 3
88⅜
C.R. RESERVE
L
C.R. CHEM.
1/8
M
C.R. RADIAL
1/8
90¼
A.N.L.
725
102⅜
C.R. RESERVE
N
C.R. CHEM.
1/8
O
C.R. RADIAL
1/8
104⅜
A.N.L.
470
116¾
C.R. RESERVE
P
C.R. CHEM.
1/8
Q
C.R. RADIAL
1/8
118½
XX
C.R. METALLURGY 3
198
XII
ANL METALLURGY 3
124¾
C.R. RESERVE
ALL THESE POSITIONS TO BE MARKED BEFORE CUTTING
CUTS TO BE MADE
16 APRIL 1953
DGK
ROD
CUTTING WILL PROCEED FROM LOWER END OF ROD
12¾ INCH SLUGS TO BE NUMBERED AND UPPER ENDS MARKED WITH ARROW BEFORE CUTTING

FIGURE 5.3.1

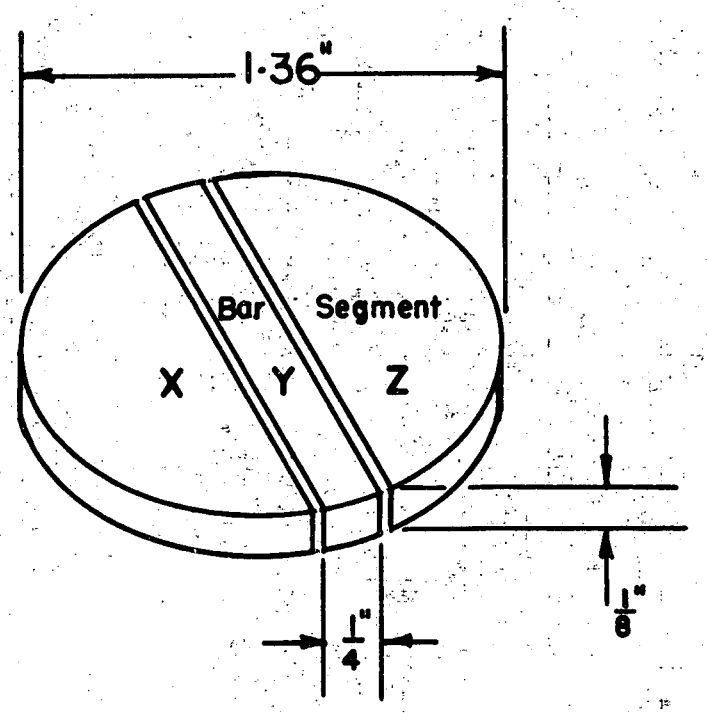

FIGURE 5.3.2

DIAMETRAL BAR CUT FROM
URANIUM CROSS-SECTIONAL DISC

---

their components. These were analysed in various ways including gamma ray counting of fission products, alpha counting, and mass spectrometry. Two of the discs have been dissolved and similarly analysed to give averages across the rod sections. In addition the depletion of U-235 has been determined by both mass spectrometry and counting techniques. This work and the results will be described in the paper by A. H. Booth and M. Lounsbury.

Some of the segments were sent to Harwell and density determinations have been made there on the material as received and also after sustained heating at various temperatures. Although there were some density differences in the material as received these are not correlated with irradiation. Heating small pieces from segment K resulted in density decreases of 2% after two days at 575°C and $3\frac{1}{2}$ to 5% after a week at 800°C.

FIGURE 5.3.3

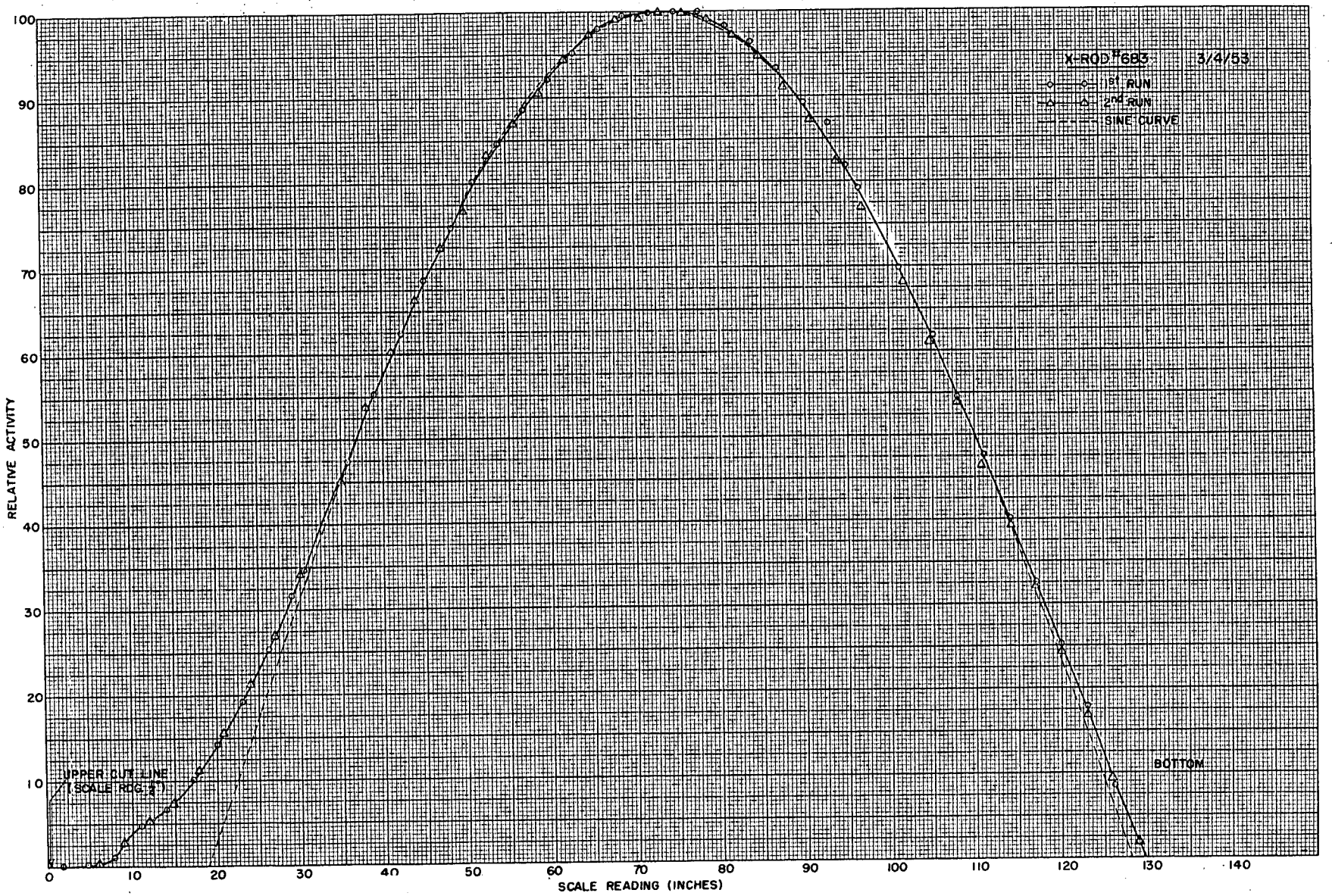
X-ROD #683 3/4/53
1st RUN
2nd RUN
SINE CURVE
RELATIVE ACTIVITY
SCALE READING (INCHES)
UPPER CUT-LINE
(SCALE REG. 27)
BOTTOM
0
10
20
30
40
50
60
70
80
90
100
110
120
130
140

As a result of all these measurements a great deal of information has been obtained. From the measurements of composition (Pu isotopes etc.) it should be possible to obtain values of effective cross-sections. Preliminary analysis has been done by G. C. Hanna who will discuss this in his paper. The involved problem of self-shielding and flux attenuation in a rod having the complex composition of the long irradiated material is being taken up by the Theoretical Physics Branch. It is expected that complete analysis of the measurements will require the solution of this problem.

REFERENCES

(1) D. G. Hurst. "Program for Rod No. 683". Report PD 256, (Chalk River, Ontario, April 1954).

(2) G. C. Hanna. "The Neutron Capture Cross Sections of Pu-239, Pu-240 and Pu-241 in NRX Pile Rods". Report PM 320, (Chalk River, Ontario, September 1954).

(3) A. H. Booth, M. Lounsbury and D. R. Mackenzie. "Radial Distribution of Cesium and Plutonium Isotopes in NRX Rod 683". Report CRC 583, (Chalk River, Ontario, November 1954).

(4) A. H. Booth and M. Lounsbury. "Radial Distribution of Cesium and Plutonium Isotopes in NRX Rod 683. Part II". Report CRC-593, (Chalk River, Ontario, May 1955).

(5) A. G. Ward. "Notes on Swing Measurements at Chicago". Report NEI-38, (Chalk River, Ontario, December 1953).

NRX Rod 683: Part II

RADIAL DISTRIBUTION OF CESIUM AND PLUTONIUM ISOTOPES

by
A. H. Booth and M. Lounsbury

INTRODUCTION

The distribution of plutonium isotopes and of Cs-137 (chosen as a measure of fission product concentration) has been investigated as a function of the radial depth into the uranium from the surface of NRX Rod 683. Analytical data, obtained by radiochemical and mass spectrometric methods, are given for Sections F, G, H, M, O, P and Q. Details of the location of these sections, and of the longitudinal variation of the irradiation at these locations are given in Part I, along with details of the cutting of the rod to provide the discs and bars required for this work. Some of the data to be presented have been reported earlier (1,2).

EXPERIMENTAL

A: Preparation of Samples

The bar was prepared for machining by placing it in a groove in a plastic disc in such a way that it was in the same relative position as it had been in the original uranium disc. It was then fixed in position with "Araldite" cement. Exact positioning of the bar was important in order that the tool should cut to a uniform depth across the face. The position of the groove in the disc was determined in the first instance by measuring the segments of the sawn disc. Assuming that the saw cuts were of uniform width, the required position of the bar could be calculated. Sometimes a small adjustment of the bar had to be made by eye, to bring its surface arc into the circumference of the plastic disc. For this, a circular plastic gauge of the same radius was held to the surface. The final check on the positioning was whether or not the first 0.002" cut of the tool exposed a bright metal surface completely across the face of the bar.

The lathe was set up in a shielded trench and operated by remote control. The tool was brought up to contact with the uranium surface, then advanced in 0.002" steps, and later in larger steps. A lucite box, into which the turnings fell, surrounded the tool and the specimen. A stream of carbon tetrachloride was directed onto the work during the machining operation and the lucite box was filled with argon to prevent the uranium turnings from igniting. If they ignited, they fused into the lucite and were difficult to wash free. After the cut, the turnings were flushed by a stream of carbon tetrachloride into a funnel leading from the lowest corner of the box, and thence into the sample tubes. The tubes were set in a circular rack which was rotated by controls outside the trench. The carbon tetrachloride was then poured out of the tubes and the turnings removed for analysis.

In the case of Sections G and P, the sample was not turned on the lathe, but rather the whole disc was dissolved, and the plutonium, cesium and uranium determinations were made on aliquots from this solution. For these two sections, sufficiently large samples were obtained so that a check on the radiochemical determination of plutonium could be made spectrophotometrically.

B: Separation Methods

The plutonium was separated from the uranium by the method described by Allison and Hart (3,4). The turnings were dissolved in 10 N HNO_3 and the solution put on a Dowex 1 anion exchange column. The column was then eluted with 10 N HNO_3. The effluent was collected in a 10 ml. volumetric flask and the washing continued until the solution was up to the mark.

In preliminary tests it was verified that more than 99.5% of the plutonium was retained on the column, while the uranium, americium, curium and cesium passed through quantitatively.

The plutonium was removed from the column with 0.5 M hydroxylamine nitrate solution. About 5 ml. of concentrated HNO_3 was put in a 25 ml. volumetric flask, and the effluent run into it, with occasional gentle swirling of the flask. The hydroxylamine decomposed rapidly in the concentrated HNO_3, and the swirling prevented the sudden evolution of a large volume of gas. When the solution was one or two millilitres below the mark, the flask was set aside and warmed under an infrared lamp until the gentle bubbling had stopped. It was then taken up to the mark with distilled water.

C: Plutonium Counting

Plutonium was determined by alpha counting of the effluent solution without further purification. Triplicate samples were evaporated on stainless steel planchets and counted in a 50% geometry counter. The geometry factor was determined by calibration against a well-defined low geometry counter. Because no appreciable solid residue remained in solution after the decomposition of the hydroxylamine, no correction for self-absorption was applied.

The result, giving the total alpha counts/min. of the combined plutonium isotopes was later resolved into isotopic components by means of the α-pulse analyzer and the mass spectrometer. In the pulse analyzer, the ratio of the counts under the 5.48 Mev peak (Pu-238) and the 5.15 Mev peak (Pu-239 and Pu-240) was determined, and from this the percent by α-counts of Pu-238 was calculated. Isotopic abundances of Pu-239, Pu-240, Pu-241 and Pu-242 were determined mass spectrometrically. The Pu-238 fraction was not observed in the mass spectrometer because of its low concentration.

For the mass spectrometer work it was found necessary to make a further purification of the plutonium solution to remove final traces of uranium as well as alkali salts, etc., accumulated from glassware and reagents. The plutonium solution was evaporated to dryness, taken up with a few drops of 10 N HNO_3, and carried through a second column process using capillary columns and very much smaller volumes of solution. The final product was evaporated to dryness in 0.5 ml. beakers.

D: Uranium Determination

In the earlier analyses the effluent from the column was evaporated, ignited at 750°C and weighed as U_3O_8. The 0.002" sample cuts weighed about 15-20 mg. and the balance could be read to ±0.05 mg., so that the precision was about ±0.5%. The uranium was set aside for possible future studies, such as U-235 burn-up. In later analyses, the uranium was determined volumetrically by titration with ceric sulphate.

E: Cesium Counting

Before evaporating the uranium solution, 0.1 ml. samples were removed for the Cs-137 determination. The 0.1 ml. sample was diluted up to 5 ml. and 0.2 ml. samples of the diluted solution were put on aluminum trays and counted by gamma scintillation in the pulse analyzer. The counts under the Cs-137 peak were totalled. In order to correct for other fission product gammas which might contribute to this total, a correction factor,

assumed constant, was established for two of the samples. This was done by carefully separating cesium from the other fission products by the standard cesium perchlorate method, and comparing the count with that of an aliquot of the original solution, which contained the cesium in unseparated form. The values found were 79.80% and 80.16%, and the factor subsequently applied to all the counts was 80.0%.

Conversion of the cesium counts to absolute disintegrations per minute was made by comparison with a standardized solution.

F: Mass Spectrometry of Plutonium

A 60°-deflection, 8"-radius mass spectrometer (5) with a theoretical resolution of 0.3% A.M.U. was used for this work. The thermionic emission ion source consisted of a tantalum filament (0.001" x 0.030" x 0.250"), mounted on pickled Kovar terminals (Stupakoff No. 9807). Ten to twenty micrograms of plutonium dissolved in 10λ of 1 N HNO_3 were dried on the filament by passing a current of about 1 amp. through it in air. In most cases the plutonium samples were small, so that it was necessary to use all of the sample for the analysis. Thus there was no opportunity to make duplicate analyses.

The loaded filament was mounted in the ion source and the mass spectrometer tube evacuated to 2×10^{-7} mm. Hg. PuO^+ ions were detected when a current of about 2.5 amps. D.C. was passed through the filament. The ions were accelerated to 7 to 10 kilovolts energy, collimated in a beam, and separated according to mass in a magnetic field of 9,000 to 11,000 gauss. The mass spectrum was scanned magnetically, and the ion currents amplified by a Vibrating Reed Electrometer (Applied Physics Corporation, Model 30) with a 2×10^{11} ohm input resistor. The output from the amplifier was fed through a calibrated attenuator system to a Speedomax Recorder (Type G).

RESULTS

A: Counting Results

The results of the Pu-238, Pu-239 plus Pu-240, and Cs-137 determinations by counting are given in Tables 5.4.1, 5.4.2 and 5.4.3 for Sections H, O and Q, and presented graphically in Figures 5.4.1, 5.4.2 and 5.4.3. Results for Sections F, G, M and P are given in Table 5.4.4. The way in which the points fit a smooth mean line suggests that the precision of the measurements may be about ±2%. This was confirmed in the few cases where it was possible to do duplicate determinations. The absolute accuracy of the results is difficult to estimate.

B: Mass Spectrometer Results

For each mass analysis, twenty to fifty spectrograms were recorded. From the measured heights of the ion current peaks, the plutonium isotopic abundances were calculated. All results were corrected for the decay of Pu-241 back to the end of the irradiation period, Sept. 24, 1951, using the value of 13.0 years for the half-life of Pu-241 determined by MacKenzie, Lounsbury and Boyd (6). These results are presented in Tables 5.4.5, 5.4.6, 5.4.7 and 5.4.8. In each case, the error quoted is the mean deviation from the mean. The accuracy of the results is about ±0.1% for 239, ±0.5% for 240, ±2% for 241 and ±15% for 242. Curves showing the isotopic abundance of Pu-240 and Pu-241 at the end of the irradiation period, as a function of radial depth, are given in Figures 5.4.4 and 5.4.5. The last column of Tables 5.4.5, 5.4.6, 5.4.7 and 5.4.8 gives the specific alpha-activity (not including Pu-238) of the plutonium samples, calculated from the mass spectrometric results. In this calculation, half-lives of 24,360 years (7), 6580 years (8) and 3.73×10^5 years (9) were used for Pu-239, Pu-240 and Pu-242 respectively.

C: Plutonium Concentrations

In Tables 5.4.9 and 5.4.10, the counting and mass spectrometric data have been combined to give the concentration, at the end of the irradiation period, of each of the plutonium isotopes in mg. per gm. of uranium for the various radial depths.

D: Uranium 235 Burnup Determinations

In the case of Sections G and P, (adjacent to Sections H and Q) where the whole disc was dissolved, the depleted uranium was mass analyzed for U-235 burnup determination. Using the value of the U-235/U-238 abundance ratio thus obtained, and the value of the same ratio for natural uranium reported previously (10), and knowing the burnup of U-238, the burnup of U-235 in Sections G and P was determined. The burnup of U-238 in these two sections was determined from the Pu/U ratio obtained by alpha-counting and mass analysis of the plutonium. This calculation neglects the destruction of U-238 by fission, but this causes a negligible error in the percent burnup of U-235. The experimental results are given in Table 5.4.11.

DISCUSSION

It will be noted that plutonium concentrations in the end of the diameter designated as Radius B, of Sections H and Q, are considerably higher (about 10%) than those at the equivalent positions at the other end of the bar, designated as Radius A. This suggests an asymmetrical flux distribution around NRX Rod 683, with the flux being higher on the B side of the rod than on the A side.

The asymmetrical flux distribution has been further investigated by gamma ray scanning of Section P and Section J. These two discs were scanned by traversing them under a 1/8" diameter hole in a lead block and counting the collimated gamma ray beam. This confirmed that there is a high and a low activity side to the rod. The diameter along which the difference is greatest (about 11%) is 30 degrees from the diameter along which the analyzed bars were cut, and is the same in both discs. The difference between the two ends, Radius A and Radius B, of the diameter along which the bars were cut is about 8 to 9%.

The analytical results for Section H, Radius B and Section Q, Radius B show anomalies of a sharp rise and fall of plutonium and cesium concentrations over a range of about 30 mil of radial depth. These anomalies are as yet unexplained.

Discussion of plutonium isotopic cross-section calculations from the above analytical data are given in Part III of this report.

REFERENCES

(1) A. H. Booth, M. Lounsbury and D. R. Mackenzie. Report CRC-583, (Chalk River, Ontario, 1954).

(2) A. H. Booth and M. Lounsbury. Report CRC-593, (Chalk River, Ontario, 1955).

(3) G. M. Allison and R. G. Hart. Report PDB-86, (Chalk River, Ontario, 1953).

(4) G. M. Allison. Report PDB-87 (Chalk River, Ontario, 1953).

(5) M. Lounsbury. Proc. Roy. Soc. Canada, 46, 128 (1952).

(6) D. R. MacKenzie, M. Lounsbury and A. W. Boyd. Phys. Rev., 90, 327 (1953).

(7) J. C. Wallman. Report UCRL-1255, (Berkeley, 1951).

(8) M. G. Inghram, et al. Phys. Rev., 83, 1250 (1951).

(9) J. P. Butler, M. Lounsbury and J. S. Merritt. Can. J. Chem. 34, 253, (1956).

(10) M. Lounsbury. Can. J. Chem. 34, 259, (1956).

TABLE 5.4.1: Counting Results

Radial Distribution of Pu Isotopes and Cs-137, Rod 683

Section H, Radius A

Radial Depth 10^{-3} in.	Total Pu α dpm/gm U	Pu-238 % of Total α	Pu-238 dpm/gm U	Pu-239 + 240 dpm/gm U	Cs-137 dpm/gm U
000-002	8.12×10^8	6.90	5.61×10^7	7.56×10^8	3.37×10^{10}
002-004	6.29	7.75	4.88	5.80	3.06
004-006	5.15	8.50	4.38	4.72	2.60
006-008	5.04	8.48	4.27	4.61	2.69
008-010	5.32			4.87	2.44
010-012	4.93			4.51	-
016-020	4.45			4.06	2.34
020-022	4.75	*	*	4.32	2.24
022-026	4.57			4.16	2.25
030-032	4.70			4.27	2.30
032-036	4.50			4.08	2.20
040-043	4.31	9.41	4.05	3.90	2.41
050-053	4.34			3.94	2.15
060-064	4.28			3.88	2.23
090-095	4.18			3.79	2.00
140-145	3.68	*	*	3.33	2.02
145-150	3.85			3.49	2.02
305-310	3.22			2.91	1.83
405-410	3.30			2.97	1.60
480-485	2.98	9.95	2.97	2.69	1.73

Section H, Radius B (opposite end of diameter)

020-024	4.69×10^8	9.44	4.43×10^7	4.25×10^8	2.40×10^{10}
030-034	3.98	10.05	4.00	3.58	1.75
040-044	4.63	10.30	4.77	4.15	2.11
050-054	4.64	10.06	4.67	4.17	2.17
060-064	4.59	10.41	4.78	4.11	2.26
070-074	5.05	10.39	5.25	4.53	2.61
080-084	5.53	12.06	6.67	4.86	2.74
090-094	4.46	11.71	5.22	3.94	2.21
150-155	4.58	10.42	4.77	4.10	2.11
200-205	3.90	10.43	4.07	3.49	1.81
300-305	3.48	10.75	3.74	3.11	1.64

* Interpolated values for these columns used to calculate next column.

TABLE 5.4.2: Counting Results

Radial Distribution of Pu Isotopes and Cs-137, Rod 683

Section 0, Radius Undetermined

Radial Depth 10^{-3} in.	Total Pu α dpm/gm U	Pu-238 % of Total α	Pu-238 dpm/gm U	Pu-239 + 240 dpm/gm U	Cs-137 dpm/gm U
000-002	5.26×10^8	4.34	2.3×10^7	5.03×10^8	1.66×10^{10}
002-004	5.10	5.07	2.6	4.84	1.60
008-010	4.71	5.60	2.6	4.45	1.52
020-022	2.78	6.16	1.7	2.61	1.32
022-024	2.89	6.43	1.9	2.70	1.46
038-040	2.72	6.22	1.7	2.55	1.27
040-045	2.56	6.24	1.6	2.40	1.20
100-105	2.50	6.66	1.7	2.33	1.23
200-205	2.40	7.10	1.7	2.23	1.25
300-305	2.25	7.03	1.6	2.09	1.14
500-505	2.16	8.27	1.8	1.98	1.14

TABLE 5.4.3: Counting Results

Radial Distribution of Pu Isotopes and Cs-137, Rod 683

Section Q, Radius A

Radial Depth 10^{-3} in.	Total Pu α dpm/gm U	Pu-238 % of Total α	Pu-238 dpm/gm U	Pu-239 + 240 dpm/gm U	Cs-137 dpm/gm U
000-002	2.45×10^8	1.86	4.55×10^6	2.40×10^8	9.31×10^9
010-012	1.59	2.73	4.33	1.54	8.46
020-022	1.48			1.44	8.12
030-032	1.46	*	*	1.42	7.47
040-042	1.45			1.41	7.65
120-125	1.21	3.44	4.14	1.16	6.97
300-305	1.18	*	*	1.14	6.43
500-505	1.15	3.54	4.07	1.11	5.63
505-775	0.98	*	*	0.94	4.69

Section Q, Radius B (opposite end of diameter)

000-020	1.97×10^8			1.93×10^8	8.61×10^9
duplicate	2.01			1.97	8.44
020-022	1.72	*	*	1.67	8.50
022-024	1.72			1.67	8.53
030-032	1.81			1.76	8.79
032-034	1.75	*	*	1.70	8.52
040-042	1.56			1.52	-
042-044	1.54			1.50	7.51

* Interpolated values for these columns used to calculate next column.

FIG. 5.4.1.

RADIAL DISTRIBUTION OF Pu-238

IN SECTIONS H, O AND Q

OF NRX ROD 683

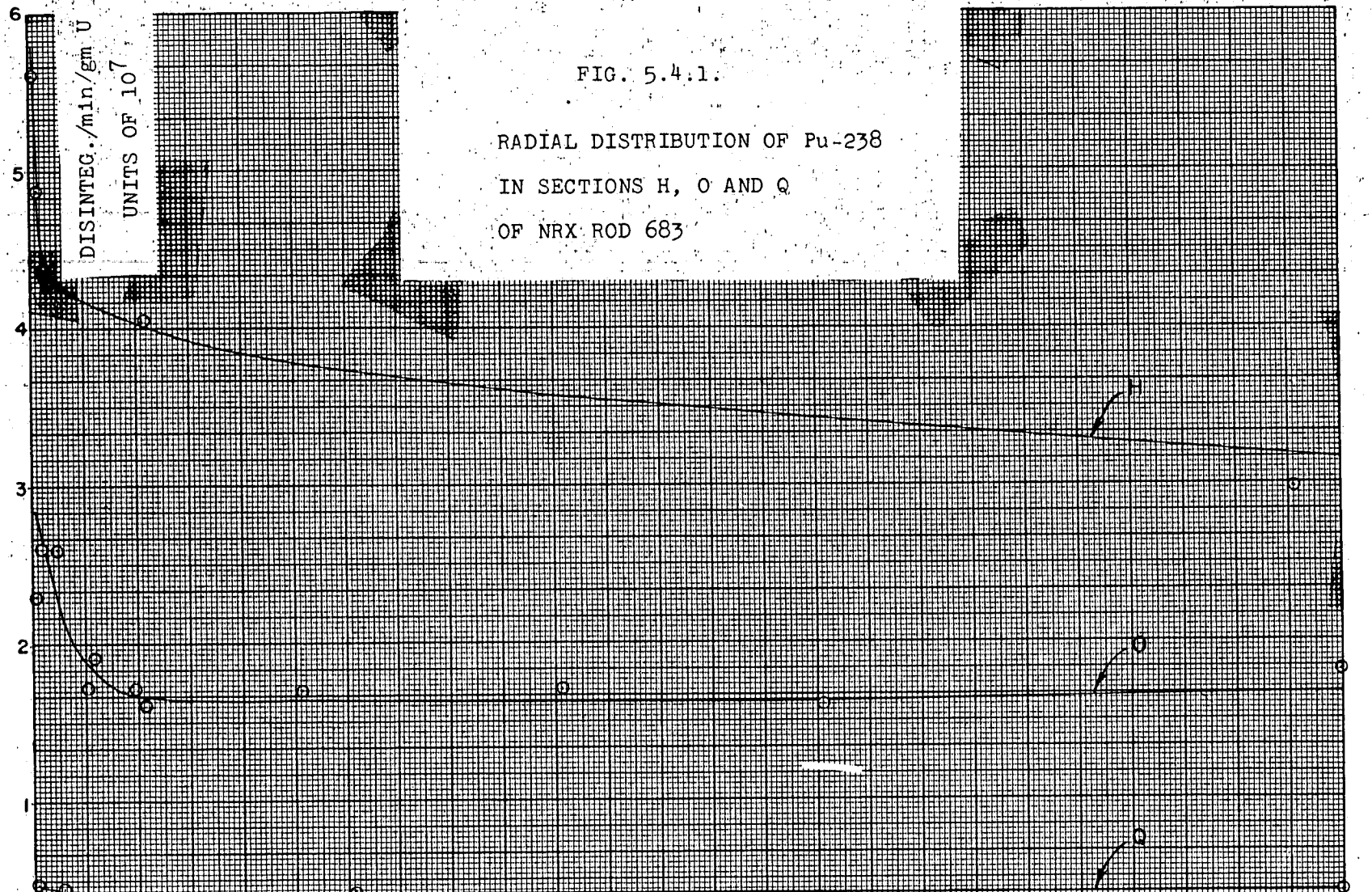

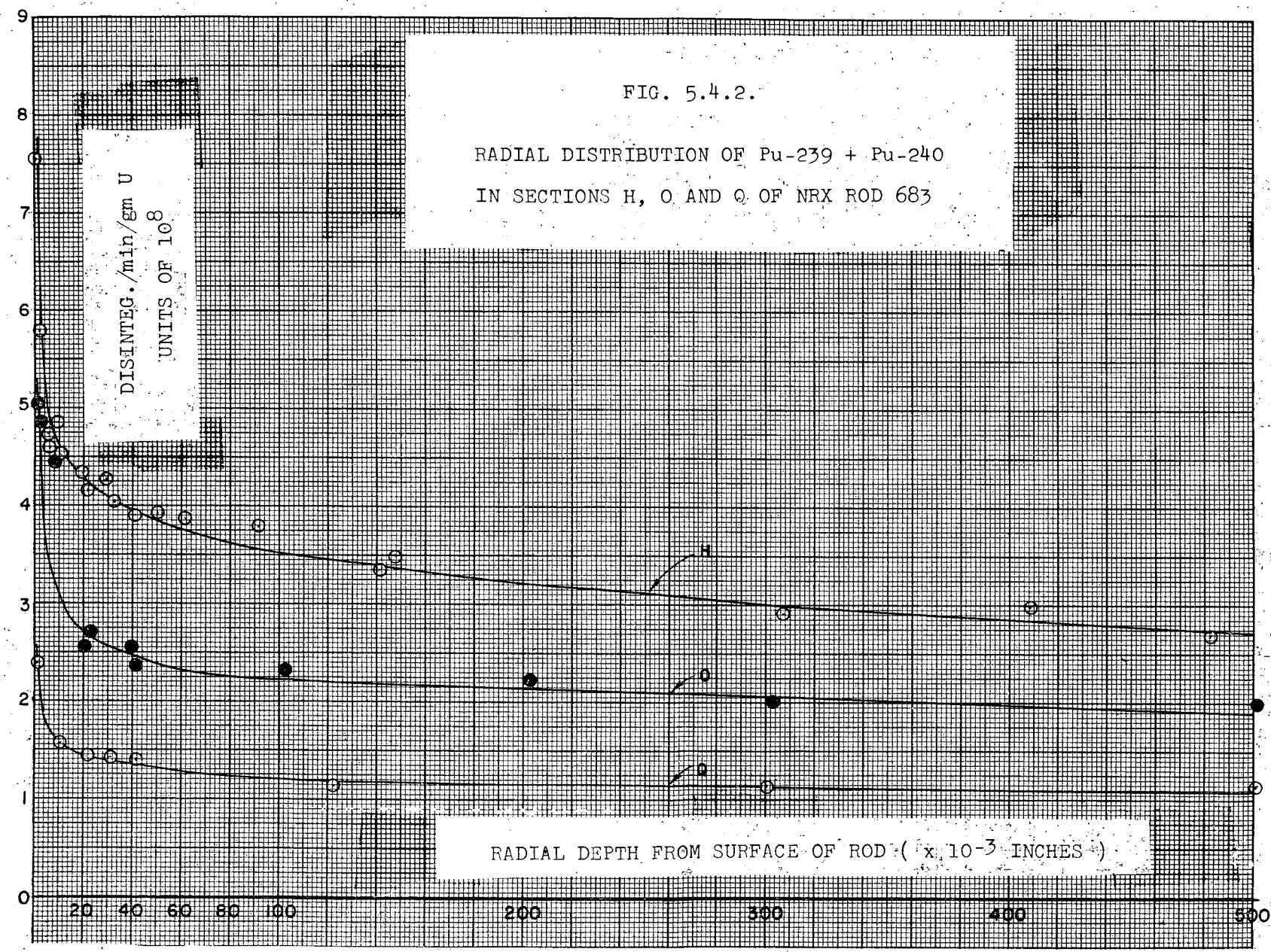
FIG. 5.4.2.
RADIAL DISTRIBUTION OF Pu-239 + Pu-240
IN SECTIONS H, O AND Q OF NRX ROD 683
DISINTEG./min/gm U
UNITS OF 10^8
RADIAL DEPTH FROM SURFACE OF ROD (x 10^{-3} INCHES)
H
O
Q
0
1
2
3
4
5
6
7
8
9
20
40
60
80
100
200
300
400
500

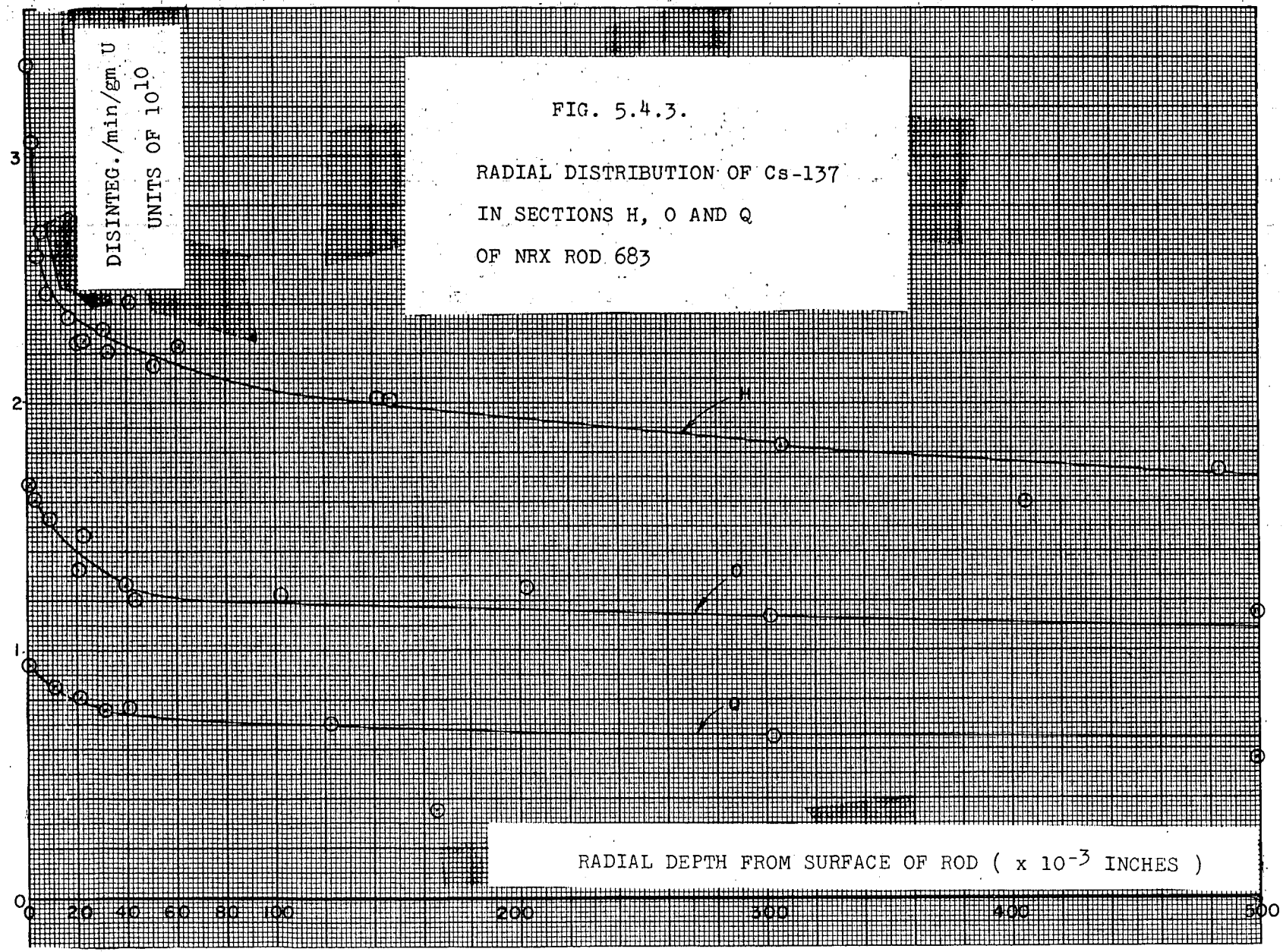
DISINTEG./min/gm U
UNITS OF 10^{10}
FIG. 5.4.3.
RADIAL DISTRIBUTION OF Cs-137
IN SECTIONS H, O AND Q
OF NRX ROD 683
H
O
Q
RADIAL DEPTH FROM SURFACE OF ROD (x 10^{-3} INCHES)
0
1
2
3
0
20
40
60
80
100
200
300
400
500

TABLE 5.4.4: Counting Results

Radial Distribution of Pu Isotopes and Cs-137, Rod 683

Section F, Radius Undetermined

Radial Depth	Total Pu	Pu-238	Pu-238	Pu-239 + 240	Cs-137
10^{-3} in.	α dpm/gm U	% of Total α	dpm/gm U	dpm/gm U	dpm/gm U
150-155	3.22×10^{8}	8.95	2.88×10^{7}	2.93×10^{8}	1.60×10^{10}
250-255	2.96	9.20	2.72	2.69	1.53
300-305	3.26	8.92	2.91	2.97	1.57
305-310	2.98	8.81	2.63	2.72	1.56
		Section G, Whole Disc			
All	3.84×10^{8}	10.20	3.92×10^{7}	3.45×10^{8}	1.98×10^{10}
		Section M, Radius B			
150-155	3.71×10^{8}	9.73	3.61×10^{7}	3.35×10^{8}	2.03×10^{10}
200-205	3.47	9.72	3.37	3.13	1.90
250-255	3.03	9.59	2.91	2.74	1.54
300-305	2.99	9.70	2.90	2.70	1.54
		Section P, Whole Disc			
All	1.27×10^{8}	3.38	4.3×10^{6}	1.23×10^{8}	5.97×10^{9}

TABLE 5.4.5: Mass Spectrometer Results

Plutonium Isotopic Abundances, Rod 683, as of Sept. 24, 1951

Section H, Radius A

Radial Depth 10^{-3} in.	Pu-239 Atom %	Pu-240 Atom %	Pu-241 Atom %	Pu-242 Atom %	Sp. α Act.* dpm/mg Pu
000-002	83.730 ±0.050	13.700 ±0.050	2.335 ±0.020	0.235 ±0.020	1.832×10^8
002-004	83.791 ±0.050	13.660 ±0.050	2.315 ±0.020	0.234 ±0.020	1.831
004-006	83.862 ±0.050	13.610 ±0.050	2.295 ±0.020	0.233 ±0.020	1.829
006-008	83.917 ±0.050	13.573 ±0.050	2.278 ±0.020	0.232 ±0.020	1.828
040-043	84.743 ±0.030	12.967 ±0.027	2.080 ±0.016	0.210 ±0.015	1.808
140-145	86.100 ±0.050	12.023 ±0.050	1.713 ±0.021	0.164 ±0.020	1.780
305-310	87.545 ±0.045	10.920 ±0.041	1.415 ±0.021	0.120 ±0.030	1.744
480-485	88.163 ±0.030	10.371 ±0.026	1.356 ±0.013	0.110 ±0.030	1.725

Section H, Radius B (opposite end of diameter)

020-024	83.134 ±0.080	14.226 ±0.080	2.396 ±0.030	0.244 ±0.030	1.850×10^8
030-034	83.088 ±0.050	14.260 ±0.050	2.408 ±0.030	0.244 ±0.020	1.851
040-044	83.699 ±0.080	13.862 ±0.070	2.217 ±0.030	0.222 ±0.005	1.839
080-084	84.414 ±0.090	13.389 ±0.090	2.002 ±0.050	0.195 ±0.018	1.825
090-094	84.672 ±0.050	13.200 ±0.050	1.940 ±0.020	0.188 ±0.007	1.819
150-155	85.512 ±0.040	12.592 ±0.036	1.743 ±0.008	0.153 ±0.004	1.800

* not including Pu-238

TABLE 5.4.6: Mass Spectrometer Results

Plutonium Isotopic Abundances, Rod 683, as of Sept. 24, 1951

Section O, Radius Undetermined

Radial Depth 10^{-3} in.	Pu-239 Atom %	Pu-240 Atom %	Pu-241 Atom %	Pu-242 Atom %	Sp. α Act.* dpm/mg Pu
000-002	88.200 ±0.080	10.330 ±0.075	1.365 ±0.020	0.105 ±0.020	1.723×10^8
004-006	88.430 ±0.052	10.136 ±0.050	1.330 ±0.010	0.104 ±0.010	1.716
016-020	88.590 ±0.054	10.022 ±0.050	1.288 ±0.015	0.100 ±0.015	1.713
034-038	88.857 ±0.079	9.803 ±0.075	1.244 ±0.020	0.096 ±0.015	1.706
090-095	89.694 ±0.033	9.147 ±0.027	1.065 ±0.018	0.094 ±0.005	1.684
250-255	90.974 ±0.023	8.142 ±0.020	0.838 ±0.010	0.046 ±0.005	1.651
300-305	91.210 ±0.052	7.945 ±0.050	0.800 ±0.010	0.045 ±0.010	1.644
350-355	91.453 ±0.026	7.725 ±0.024	0.777 ±0.008	0.045 ±0.005	1.636
500-505	91.881 ±0.077	7.376 ±0.075	0.702 ±0.015	0.041 ±0.010	1.625

* not including Pu-238

TABLE 5.4.7: Mass Spectrometer Results

Plutonium Isotopic Abundances, Rod 683, as of Sept. 24, 1951

Section Q, Radius A

Radial Depth 10^{-3} in.	Pu-239 Atom %	Pu-240 Atom %	Pu-241 Atom %	Sp. α Act.* dpm/mg Pu
000-002	94.043 ±0.050	5.571 ±0.050	0.386 ±0.018	1.563×10^8
020-022	94.297 ±0.018	5.320 ±0.016	0.383 ±0.005	1.554
040-042	94.611 ±0.030	5.058 ±0.022	0.331 ±0.010	1.545
120-125	95.046 ±0.018	4.626 ±0.018	0.328 ±0.015	1.530
300-305	95.401 ±0.020	4.286 ±0.017	0.313 ±0.005	1.517
500-505	95.620 ±0.010	4.080 ±0.010	0.300 ±0.005	1.510

Section Q, Radius B (opposite end of diameter)

000-020	93.171 ±0.030	6.273 ±0.027	0.556 ±0.015	1.587×10^8
022-024	93.267 ±0.075	6.185 ±0.075	0.548 ±0.035	1.584
030-032	93.496 ±0.060	5.980 ±0.058	0.524 ±0.015	1.576
040-042	93.620 ±0.060	5.927 ±0.060	0.453 ±0.022	1.575

* not including Pu-238

TABLE 5.4.8: Mass Spectrometer Results

Plutonium Isotopic Abundances, Rod 683, as of Sept. 24, 1951

Section F, Radius Undetermined

Radial Depth 10^{-3} in.	Pu-239 Atom %	Pu-240 Atom %	Pu-241 Atom %	Pu-242 Atom %	Sp. α Act.* dpm/mg Pu
150-155	87.685 ±0.040	10.805 ±0.040	1.414 ±0.020	0.096 ±0.010	1.740×10^8
250-255	88.561 ±0.030	10.054 ±0.025	1.295 ±0.020	0.090 ±0.018	1.714
300-305	88.990 ±0.050	9.755 ±0.040	1.175 ±0.030	0.080 ±0.020	1.705
305-310	89.022 ±0.050	9.748 ±0.040	1.150 ±0.020	0.080 ±0.020	1.705

Section G, Whole Disc

all	86.239 ±0.050	11.944 ±0.044	1.669 ±0.024	0.148 ±0.006	1.777×10^8

Section M, Radius B

150-155	86.355 ±0.050	11.884 ±0.042	1.619 ±0.014	0.142 ±0.010	1.776×10^8
200-205	86.822 ±0.050	11.531 ±0.040	1.517 ±0.020	0.130 ±0.010	1.765
250-255	87.351 ±0.050	11.122 ±0.050	1.411 ±0.020	0.116 ±0.010	1.751
300-305	87.886 ±0.040	10.679 ±0.030	1.329 ±0.022	0.106 ±0.010	1.736

Section P, Whole Disc

all	94.859 0.034	4.814 0.032	0.327 0.010	--	1.536×10^8

* not including Pu-238

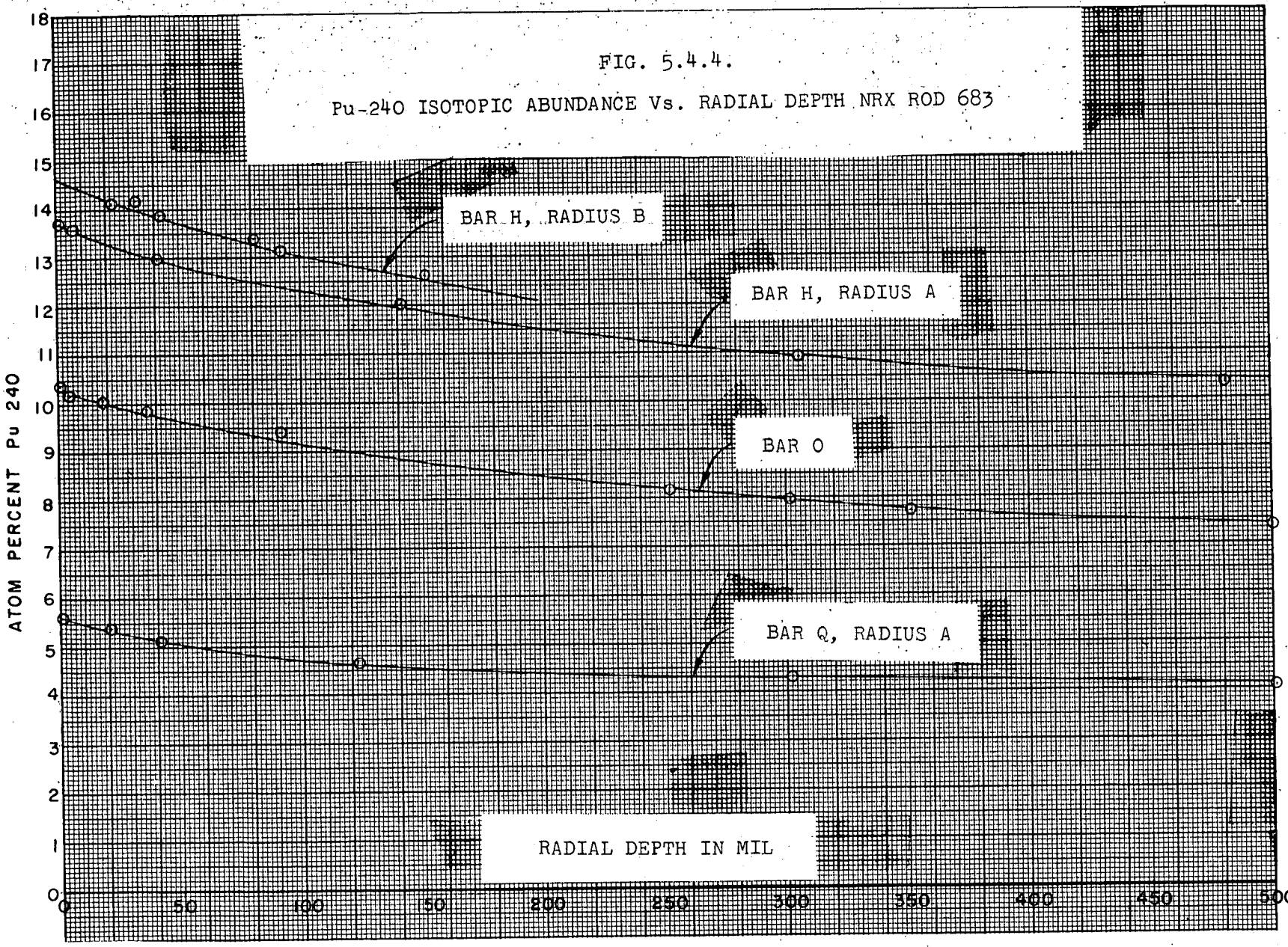
FIG. 5.4.4.
Pu-240 ISOTOPIC ABUNDANCE Vs. RADIAL DEPTH NRX ROD 683
BAR H, RADIUS B
BAR H, RADIUS A
BAR O
BAR Q, RADIUS A
ATOM PERCENT Pu 240
RADIAL DEPTH IN MIL
0
1
2
3
4
5
6
7
8
9
10
11
12
13
14
15
16
17
18
50
100
150
200
250
300
350
400
450
500

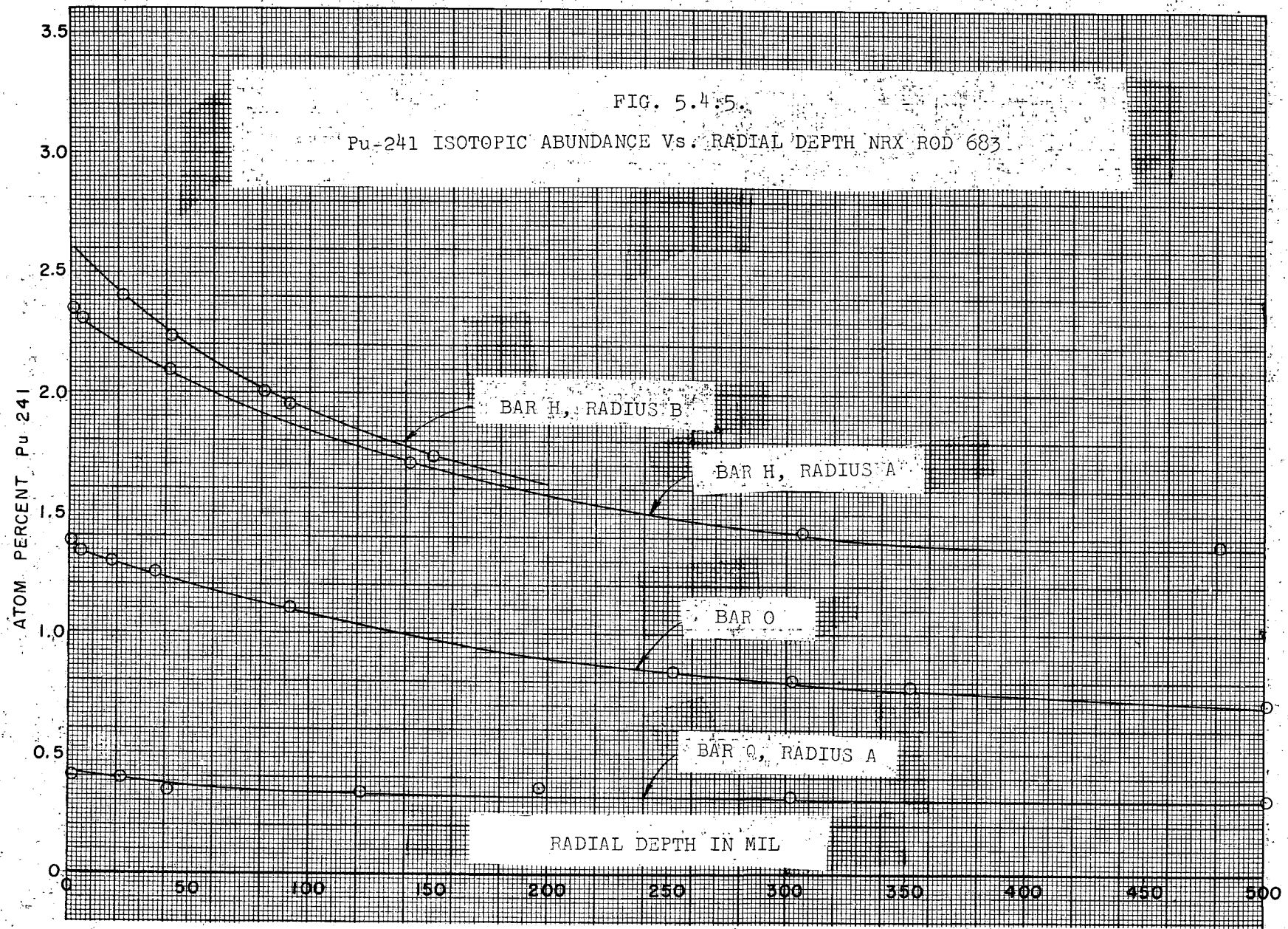
FIG. 5.4.5.
Pu-241 ISOTOPIC ABUNDANCE Vs. RADIAL DEPTH NRX ROD 683
ATOM PERCENT Pu 241
3.5
3.0
2.5
2.0
1.5
1.0
0.5
0
BAR H, RADIUS B
BAR H, RADIUS A
BAR O
BAR O, RADIUS A
RADIAL DEPTH IN MIL
0
50
100
150
200
250
300
350
400
450
500

TABLE 5.4.9:

Radial Concentration of Pu Isotopes, Rod 683, as of Sept. 24, 1951

Section H, Radius A

Radial Depth 10^{-3} in.	Total Pu mg/gm U	Pu-239 mg/gm U	Pu-240 mg/gm U	Pu-241 mg/gm U	Pu-242 mg/gm U
000-002	4.128	3.456	0.567	0.096	0.010
002-004	3.169	2.655	0.433	0.073	0.007
004-006	2.581	2.164	0.351	0.059	0.006
006-008	2.522	2.116	0.342	0.057	0.006
040-043	2.157	1.828	0.280	0.045	0.005
140-145	1.871	1.611	0.225	0.032	0.003
305-310	1.669	1.461	0.182	0.024	0.002
480-485	1.560	1.375	0.162	0.021	0.002

Section H, Radius B

020-024	2.297	1.910	0.327	0.055	0.006
030-034	1.934	1.607	0.276	0.047	0.005
040-044	2.256	1.889	0.313	0.050	0.005
080-084	2.663	2.248	0.357	0.053	0.005
090-094	2.166	1.834	0.286	0.042	0.004
150-155	2.278	1.948	0.287	0.040	0.003

Section Q, Radius A

000-002	1.535	1.444	0.086	0.006	--
020-022	0.927	0.874	0.049	0.004	--
040-042	0.913	0.863	0.046	0.003	--
120-125	0.758	0.721	0.035	0.003	--
300-305	0.751	0.717	0.032	0.002	--
500-505	0.735	0.703	0.030	0.002	--

Section Q, Radius B

000-020	1.216	1.133	0.076	0.007	--
022-024	1.055	0.984	0.065	0.006	--
030-032	1.117	1.044	0.067	0.006	--
040-042	0.965	0.903	0.057	0.004	--

TABLE 5.4.10:

Radial Concentration of Pu Isotopes, Rod 683, as of Sept. 24, 1951

Section F, Radius Undetermined

Radial Depth 10^{-3} in.	Total Pu mg/gm U	Pu-239 mg/gm U	Pu-240 mg/gm U	Pu-241 mg/gm U	Pu-242 mg/gm U
150-155	1.684	1.477	0.182	0.024	0.002
250-255	1.569	1.390	0.158	0.020	0.001
300-305	1.742	1.550	0.170	0.021	0.001
305-310	1.595	1.420	0.156	0.018	0.001

Section G, Whole Disc

all	1.941	1.674	0.232	0.032	0.003
all	1.96	(spectrophotometric determination)			

Section M, Radius B

150-155	1.886	1.629	0.244	0.031	0.003
200-205	1.774	1.540	0.205	0.027	0.002
250-255	1.565	1.367	0.174	0.022	0.002
300-305	1.555	1.366	0.166	0.021	0.002

Section P, Whole Disc

all	0.798	0.757	0.038	0.003	--
all	0.796	(spectrophotometric determination)			

TABLE 5.4.11:

U-235 Burnup Determinations, Rod 683

	Section G	Section P
Initial Ratio U-235/U-238	$(0.7257 \pm 0.0007) \times 10^{-2}$	$(0.7257 \pm 0.0007) \times 10^{-2}$
Final Ratio U-235/U-238	$(0.4632 \pm 0.0011) \times 10^{-2}$	$(0.6175 \pm 0.0014) \times 10^{-2}$
% Burnup U-238	0.195	0.0798
% Burnup U-235	36.30 ± 0.16	14.96 ± 0.21

NRX Rod 683: Part III

INTERPRETATION OF MEASUREMENTS

by
G. C. Hanna

Revised June, 1956

Contents

A. Introduction - Objectives, Assumptions, and Limitations

A complete interpretation of the experimental measurements of the composition of rod 683 will provide data on how the rates of production of the various plutonium isotopes vary with depth in the rod and with degree of irradiation. The dependence on irradiation is obtained from a comparison between samples from different points along the rod, since it has been established (CRP-396) that the initial cadmium ratio does not change appreciably along the rod, at least over the length so far studied. Therefore differences between samples arise solely from the change in neutron spectrum produced by changes in the neutron absorption properties of the rod as the irradiation increases.

It is not possible to say how closely the results from rod 683 will apply to the hypothetical "average" rod in NRX since no measurements of the cadmium ratio have been made across the pile. Rod 683 received about one third of its irradiation in an intermediate position (D12, ring 10, 79 cm radius) and two thirds in an outlying position (F26, ring 16, 105 cm radius), where it was one of the penultimate rods of the core. In both positions it was surrounded by five normal X rods and one vacancy, which is the average environment of an NRX rod. On the other hand, the large discrepancy between expected and measured irradiation levels (Section C below) and the anomalously high flux gradient across the rod both suggest that its environment may well not have been typical.

It is necessary to assume at least for the present that the distribution of the various isotopes has not been affected by diffusion during the irradiation. This effect is expected to increase rapidly with temperature, and therefore its importance, at a given depth in the rod, might well increase quite suddenly in the series of successively more heavily irradiated discs. Therefore when, with more detailed flux data than are now available, the radial variation of effective cross sections can be evaluated accurately as a function of irradiation, it may be possible to settle this point on the basis of whether or not a trend that is apparent over a modest irradiation range is more or less sharply modified at higher levels. So far there has been no compelling suggestion that diffusion effects are significant.

Even with the assumption that diffusion effects are negligible, a complete interpretation of the data will be a difficult problem. Ideally, one would start with known data on cross sections as a function of neutron energy, and the spatial distribution of neutrons of different energies in a pile rod, and calculate the rates of the various reactions in all parts of the rod. As the irradiation proceeded it would be necessary, at suitably spaced intervals, to modify the neutron-flux distribution in accordance with the changing concentrations of the various nuclides. The calculation of the modified neutron distribution would be difficult, particularly because of the non-uniform composition of the rod. A comparison of the calculated

concentrations with the experimental measurements at the appropriate stages would then give more accurate values of those input data that were initially known only approximately. The Theoretical Physics Branch is working on such an analysis, and in view of their expected contribution the present interpretation has been kept as simple as possible.

The present analysis proceeds in the following way. In principle, for every sample from the rod, the integrated flux is known either directly from U^{235} depletion measurements or, after correction for plutonium fission and appropriate normalization, from the Cs^{137} counting data. It is assumed that U^{235} behaves sufficiently like a (1/v) neutron absorber that its disappearance measures the time integral of the neutron density. The integrated flux is therefore $nv_0 = \int_0^\infty n'(v)\, dv\, v_0$, and the cross sections of other nuclides that are to be used with this flux are therefore "effective" cross sections equal to $\int_0^\infty \sigma(v)\, v\, n'(v)\, dv/nv_0$. $n'(v)$ is the distribution function for neutron density in terms of velocity v, n is the total neutron density, and $v_0 = 2200$ m/sec (see Westcott, RPI-11). The aim of the analysis is to deduce such effective cross section values (henceforth the term effective will be omitted) from the experimental data: their variations with depth in the rod and irradiation level will reflect the corresponding changes in neutron spectrum.

Cross sections can be calculated in a straightforward way only if, in a given sample, the neutron spectrum remains unchanged

during the irradiation, and the present analysis makes this assumption. The results obtained - cross-section values that, in general, change appreciably with irradiation - show immediately that the assumption is invalid. The cross-section values obtained are more or less complicated "averages" over the duration of the irradiation: what is required is the behaviour of the "instantaneous" values as a function of irradiation. It can be shown that this information can be obtained, fairly simply and with adequate accuracy, from the behaviour of the "average" value provided that the irradiation dependence is not too pronounced. This problem is discussed at length in the Appendix with particular reference to the irradiation dependence of the capture cross section of Pu^{239}. Neutron capture in Pu^{240} is too strongly influenced by self shielding to be treated adequately by this method, but it is shown that its complicated behaviour does not affect seriously the interpretation of the cross-section values obtained for the other nuclides.

A practical difficulty remains. The Cs^{137} data have been found to be unreliable, and very few measurements of U^{235} depletion have been made. Thus for most samples the estimates of total integrated flux are not very accurate, and a quantitative interpretation of the variation of cross-section values with depth and irradiation level cannot yet be made.

Accurate measurements, including very precise U^{235} depletion data, have been made on complete discs. Their interpretation demands a knowledge of the neutron flux distribution across the

discs, but, fortunately, only an approximate one. The effect of a non-uniform flux distribution on the n^{th} order neutron reaction is given to a first order by the parameter $R_n = \overline{\phi^n}/(\bar{\phi})^n$. Since, in the present case, $R_2 \doteqdot 1.02$, $R_3 \doteqdot 1.06$, $R_4 \doteqdot 1.12$, it is evident that small uncertainties in the flux distribution will not introduce significant errors. It will be appreciated however that in this case the cross-section value obtained is that of the appropriately weighted average across the disc. This matter is considered more fully in the Appendix.

B. Measurements of Integrated Flux by U^{235} Depletion

At Chalk River the depletion of U^{235} has so far been measured in only two samples, the complete discs G (near the centre of the rod) and P (near one end). Mass spectrometer analysis gave values of 36.30±0.16 and 14.98±0.21 respectively for the percentage of the initial U^{235} destroyed. Westcott (TNCC(CAN)-1) has calculated that the absorption cross section of U^{235} is 687 barns for a maxwellian spectrum at 20° C. An earlier estimate of 685 barns has been used throughout the present work. This gives, for the average across the rod of the integrated neutron flux, 0.6611±0.0036 n's/kb in G and 0.2373±0.0036 n's/kb in P. Neglect of the non-uniformity of the flux distribution would reduce these figures by, respectively, 0.4 percent and 0.14 percent.

A method of measuring U^{235} depletion by counting methods is being developed but has encountered several difficulties.

So far only the same two samples have been measured, with results in satisfactory agreement with those of the mass spectrometer but of somewhat inferior accuracy. As a by-product of some of the alpha counting done during this work, the depletion of U^{234} in sample G was measured and a value of 147±9 barns obtained for the total absorption cross section of U^{234}. This is to be compared with the values of 72 and 92 barns quoted in BNL 325 for "pile neutrons". A measurement of the U^{236} alpha activity of sample G gave α ($= \sigma_c/\sigma_f$) in U^{235} = 0.189±0.010: the accepted value for 2200 m/sec neutrons is 0.184±0.008 (BNL 325).

The Argonne National Laboratory has measured the depletion of U^{235} as a function of rod radius in disc R. It should be noted that their samples were obtained by controlled dissolving and therefore represent an average around the rod, in contrast with the Chalk River radial distribution work, which used samples from diametrical bars and showed the existence of a flux gradient across the rod.

The A.N.L. results on the U^{235} depletion, expressed as irradiations in neutrons per kilobarn, are shown in Fig. 5.5.1. The U^{236} content of each sample is consistent with a value of α = 0.198±0.004 except for the sample at 257 mil depth, where this value of α would give a five percent higher irradiation (shown by the cross in Fig. 5.5.1). The solid-line curve has been drawn freehand without any attempt to fit the data to a theoretical expression and is certainly not a unique

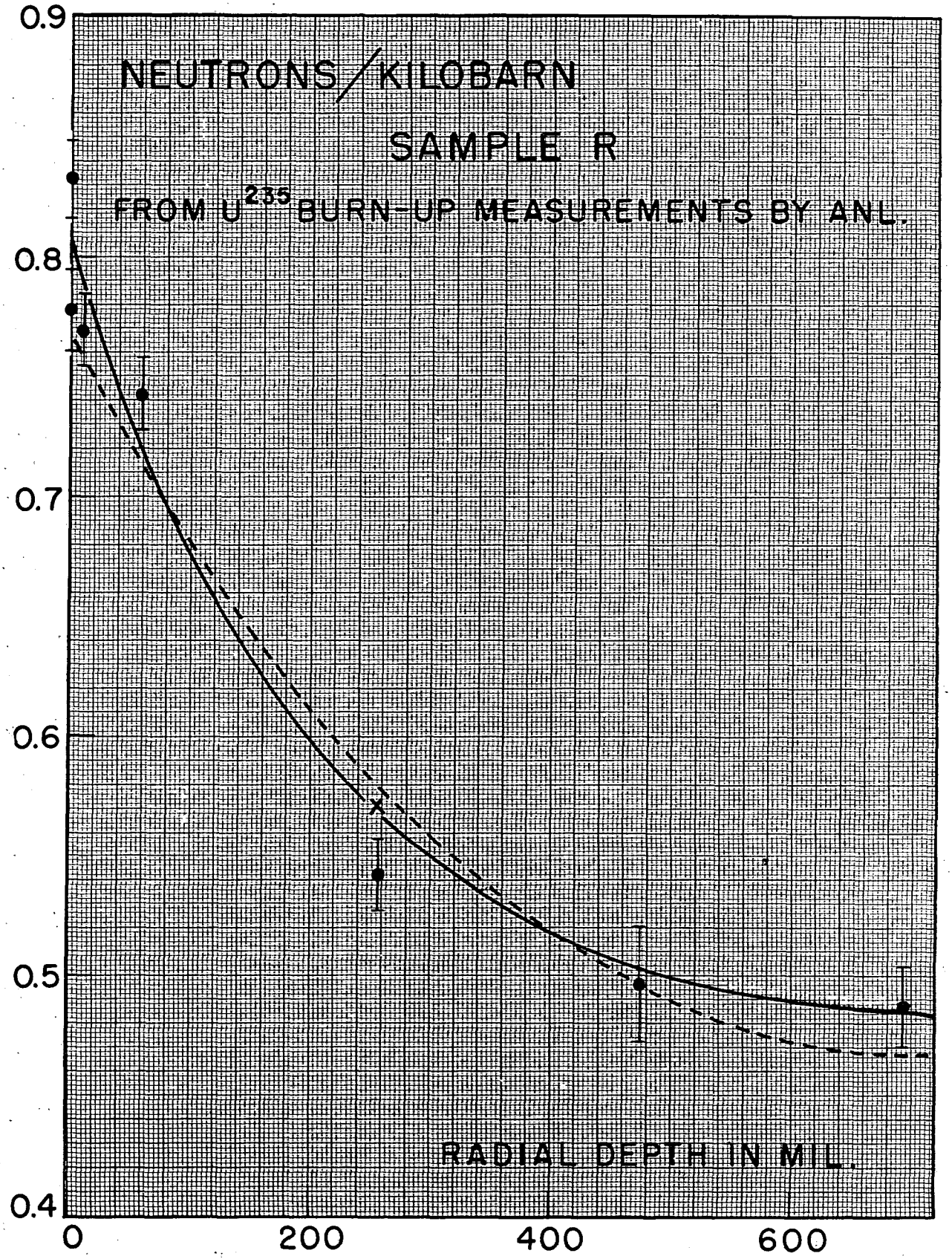

Fig. 5.5.1. Radial distribution of integrated neutron flux in sample R from U^{235} depletion measurements by A.N.L. The point X is calculated from the U^{236} content. The solid curve is drawn freehand; the dotted curve is the function $I_0(\varkappa r)$ with $\varkappa = 0.833$ cm^{-1} normalized to the same average flux.

"best fit". However it probably represents the true situation with an accuracy of two or three percent. The dotted curve is the Bessel function $I_0(\varkappa r)$ with $\varkappa = 0.833$ cm^{-1} normalized to give the same average irradiation as the solid curve (0.611 neutrons/kilobarn). This value of $\varkappa$ was obtained by Hone from a least-squares fit of experimental data on the flux distribution across a fresh rod. These data showed no systematic departure from the Bessel function: the difference in the present case is presumably the result of a change in the neutron absorption properties of the rod following irradiation.

In the absence of any other reliable flux distribution data, the solid curve of Fig. 5.5.1, corrected for the gradient across the rod (Part II), has been assumed to apply to discs of all irradiation levels: it will be referred to as the A.N.L. distribution. The gradient has been allowed for by multiplying the curve by $(1 + 0.045r/a)$ where a is the rod radius and r (negative for radius "A" and positive for "B") is the radius of the sample. The use of the A.N.L. distribution is reasonable for discs H, M, and F, which had irradiations very similar to that of R, but for O, and even more for Q, it may well be misleading. It might be thought that the fresh-rod Bessel function would be a better approximation for Q at least, but the evidence from neutron capture in Pu^{239} is against this. Apart from R, absolute values of the integrated flux are available only for H and Q, from the measured averages in the adjacent discs G and P.

An attempt was made to obtain a more realistic flux distribution for Q from the Cs^{137} data. Fig. 5.5.2 shows the data from Q(A) and H(A) as a comparison between the measured Cs^{137} activity, corrected for the contribution from plutonium fission and the expected activity from U^{235} fission calculated from the A.N.L. flux distribution. The measured corrected activity was only about 70 percent of that expected, and the data have been arbitrarily normalized (using the same normalizing factor for both Q(A) and H(A)) to give an average ratio of about unity in H(A). The data are not very sensitive to the correction for plutonium fission, which amounts to roughly 15 percent in H; an increase of 20 percent in this correction would decrease the ratio $\overline{H}/\overline{Q}$ by about two percent and H(20 mil)/H(centre) by the same amount.

The scatter of the points is too great to allow any definite conclusions to be drawn. There is no evidence that the A.N.L. distribution does not apply to H(A), except for the curious skin of Cs^{137}, which remains unexplained (an increase of a factor of three in the correction for plutonium fission would be required to "remove" it). The data from Q(A) suggest that, between 0 and 200 mil depth, the flux is lower than that predicted by the A.N.L. distribution, a feature which is also suggested by the Pu^{239} and Pu^{240} concentrations.

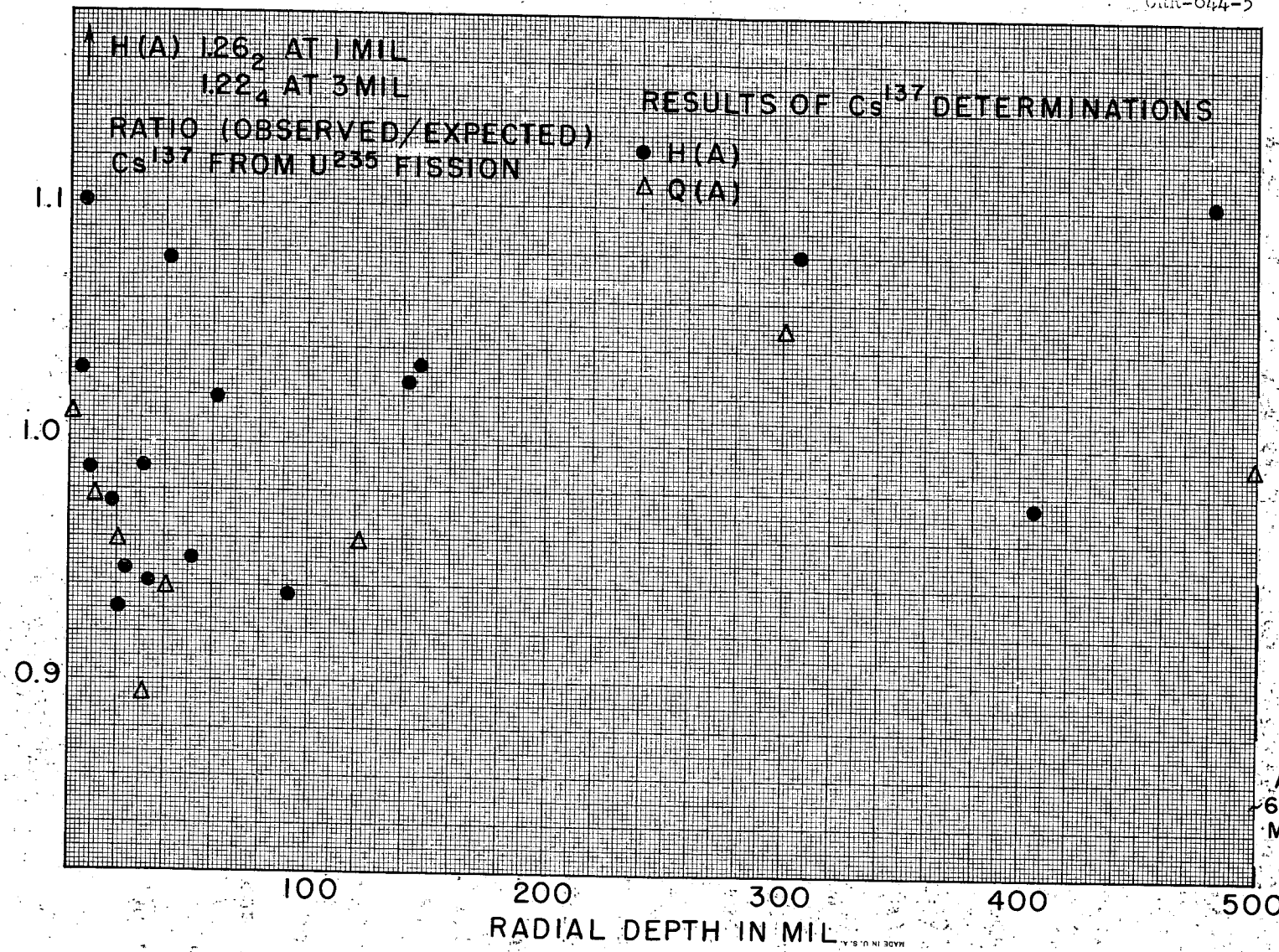

Fig. 5.5.2. Results of Cs^{137} counting expressed as the ratio of observed Cs^{137} from U^{235} fission to that calculated using the A.N.L. flux distribution corrected for the gradient across the rod. The normalization is arbitrary but the same for Q(A) and H(A). The point at ~600 mil refers to a thick sample 505 to 775 mil below the surface of Q(A).

C. Comparison with Expected Irradiation Levels

The expected irradiation of the various discs may be calculated from the integrated pile power if the fraction dissipated in a given rod position and the flux distribution along the rod are known.

The "output fractions" (Paper I) are based on a flux distribution measured at low power in a fresh reactor. Recent measurements of the temperature rise of individual rods, averaging over all rods at a given distance from the centre of the pile, showed that these output fractions are correct within a few percent. On the other hand, these measurements revealed a quite unexpected azimuthal flux variation, but there is no evidence whether such a variation was present during the irradiation of rod 683. The rod had a normal complement of nearest neighbours, and no local anomaly in flux is expected. The observed shortening of the rod (Paper I) agreed with that expected from the calculated total irradiation, but a discrepancy of 10 to 15 percent would not be considered significant.*

The variation of gamma-ray activity along the rod was measured by Henderson and Tunnicliffe (Paper I). The activity is due mainly to the longer lived fission products of U^{235}

---

* The writer is indebted to Dr. W.M. Barss for access to his unpublished data and for helpful discussions on this point.

and Pu^{239}, with a small contribution from fast fission in U^{238} and a quite negligible one from Pu^{241}, both of which have been ignored. The principal uncertainty in calculating the irradiation from the gamma activity is the relative fission yields of the relevant activities. Assuming that the main activity is Cs^{137}, which has a fission yield ratio Pu/U = 4.9%/6.08% = 0.81, it is calculated that the ratio of irradiation to gamma activity increases essentially linearly with irradiation and is 3±3 percent higher at 0.6 neutrons/kilobarn than at zero irradiation. The error quoted corresponds to an error of ±20 percent in the ratio of fission yields. The calculated irradiation distribution is very close to the expected sine curve.

The calculated and measured irradiations for P, R, and G are shown in the table below.

Table 5.5.1

Sample	P	R	G	Ratio P/R/G
Calculated irradiation (neutrons/kilobarn)	0.21_5	0.74_7	0.75_8	$0.28_4/0.98_3/1$
Irradiation from U^{235} depletion (neutrons/kilobarn)	0.23_7	0.61_1	0.661	$0.35_8/0.92_5/1$

The analysis of the other discs (Q, O, F, M, and H) has shown that there was no confusion of samples, and that G and R are from the maximum flux region of the rod. The discrepancy (~15 percent) between the calculated and measured irradiations of G and R therefore implies that the actual power dissipated

in the rod in at least one of its irradiation positions (F26, D12) was less than that given by the expected output fraction, perhaps as the result of a local anomaly due to uneven loading. Although in both cases the rod had a normal complement of nearest neighbours, the presence of a local anomaly is also suggested by the experimentally observed flux gradient across the rod, which is twice as great as that expected from the gross flux distribution across the pile. The observed shortening rates of neighbouring rods also suggest that there was an abnormally high flux gradient across the irradiation position F26 (no data are available for D12).

The serious discrepancies between the calculated and measured irradiation ratios P/G and R/G, however, depend only on the gamma-ray scan measurement and its interpretation. Either this is completely wrong - and the longitudinal flux variation is much flatter than the expected sine curve - or there have been errors in the cutting procedure.

D. Plutonium Production

The accurate measurements of the ratio (Pu^{239}/uranium) and of the U^{235} depletion in the complete discs P and G give values of the average over the rod area of the initial conversion ratio (the number of Pu^{239} atoms formed per U^{235} atom destroyed) and the initial production factor (gm Pu per MWD). The non-uniformity of the flux distribution has been allowed for: neglect of this would give values for the conversion factor

and production rate that are too low by about 0.6 percent in G and 0.2 percent in P. The values shown in Table 5.5.2 were derived on the following assumptions: σ_9, the total cross section of Pu^{239}, is 1300 barns (corresponding to σ_{c9} = 430 barns (cf. Section E) and σ_{f9} = 870 barns, a value calculated by Westcott for an NRX rod), E_f = 200 Mev/fission, ϵ = 1.035, and α = 0.184; the last three quantities are required only for the calculation of the production rate.

Table 5.5.2

Sample	P	G
Irradiation (neutrons/kilobarn (MWD/10^6 gm	0.2373±0.0036 970	0.6611±0.0035 2740
Initial conversion factor	0.753±0.008	0.769±0.007
Initial production rate (gm/MWD)	0.901±0.010	0.920±0.008

A decrease of 100 barns in the value assumed for σ_9 would decrease the calculated values of conversion factors and production rates by about one percent in P and three percent in G. A very rough calculation of the expected change in rod blackness (see Appendix II(iii)) suggests that the apparent initial conversion rate should increase by only ~0.2 percent between P and G, so that, in principle, with a refined estimate of the effects of the change in blackness, a fairly accurate value of σ_9 should be available from these data. The experimental errors are however too large at present to give a worthwhile value.

Barss has made a careful study of the experimental data on the plutonium content of NRX rods as a function of integrated pile power. He concludes (NEI-27) that the initial production rate is 0.90_4 gm/MWD with an accuracy of about ±2 percent.

It should be noted that with σ_5 = 685 barns a conversion factor of 0.76±0.01 corresponds to a value of σ_8, the capture cross section of U^{238}, equal to 3.78±0.04 barns. Since the thermal neutron capture cross section of U^{238} is 2.75±0.04 barns (BNL 325), it appears that 27.2±1.4 percent of the plutonium is produced by resonance capture.

The experimental data on the radial distribution of the plutonium have been examined in detail only for H(A) and Q(A). Values of σ_8 have been calculated from the A.N.L. flux distribution (corrected for gradient as described in Section B and with absolute values obtained from G and P). It is assumed that the ratio of fission to capture cross sections in Pu^{239} is constant across the rod and equal to 870/425. The results are shown in Fig. 5.5.3. The data of H(A) indicate that the skin of plutonium formed by the surface absorption of resonance neutrons contributes about 2.5 percent of the total plutonium production.

The average value of σ_8 in H(A) is evidently in reasonable agreement with the value of 3.8 barns obtained from G. The data from Q(A) are rather ragged, but there is a suggestion that between 0 and 200 mil all the Q(A) points are low. This may well indicate a lower flux than that deduced from the

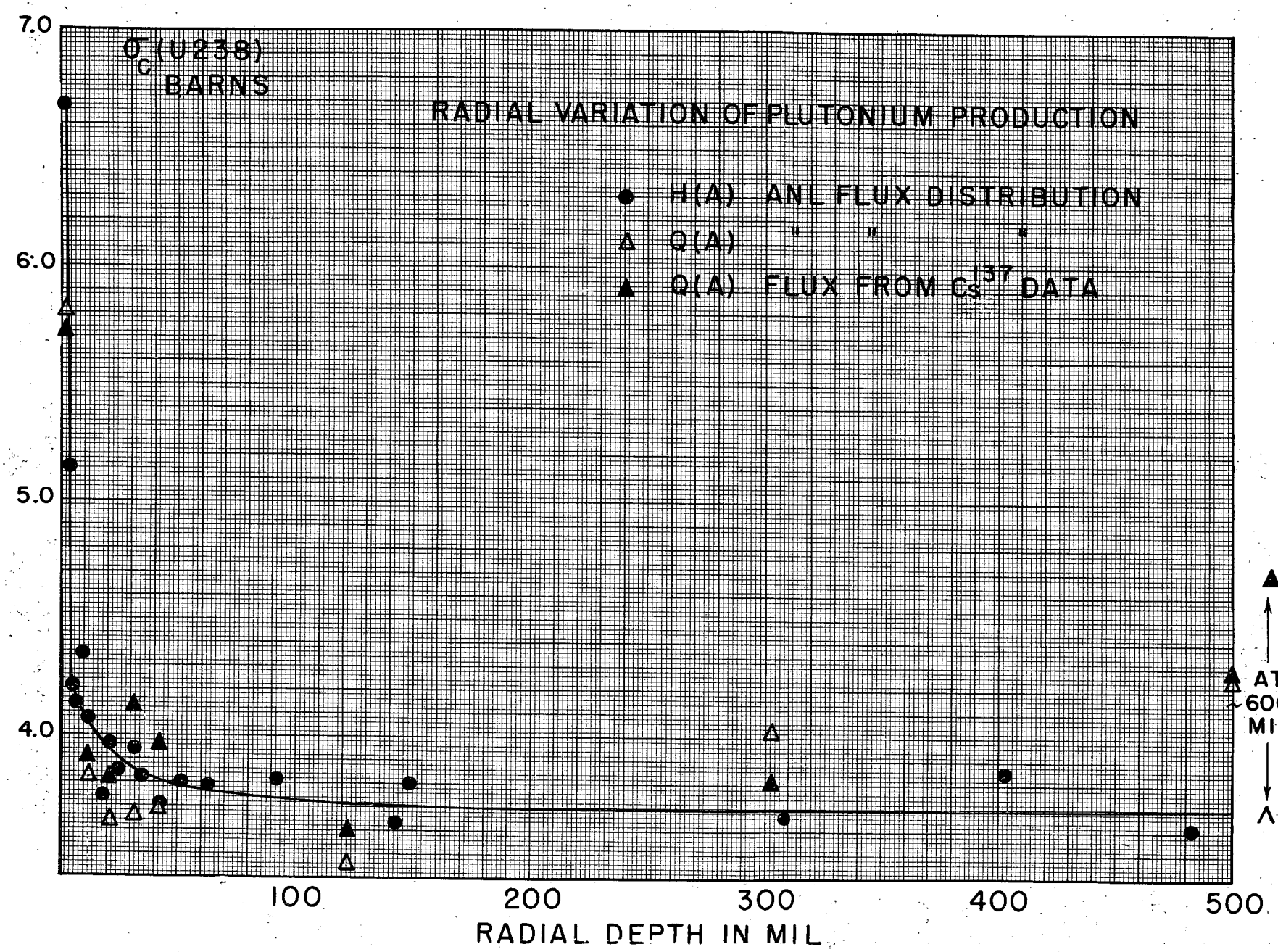

Fig. 5.5.3. The effective capture cross section of U^{238} as a function of radial depth in Q(A) and H(A).

A.N.L. distribution, a feature that was also suggested by the Cs^{137} results. The solid triangles of Fig. 5.5.3 are the values of σ_8 calculated from the Q(A) measurements with flux data obtained from the Cs^{137} activities corrected and normalized as for Fig. 5.5.2 (Section B). The agreement with the H(A) data is much better in the 0 to 200 mil region: towards the centre of the rod the data are too meagre for any definite conclusions to be drawn.

E. The Capture Cross Sections of Pu^{239}, Pu^{240}, and Pu^{241}

Values of σ_{c9}, σ_0, and σ_{c1} have been calculated from the data of G and P on the assumption that σ_9 = 1300 barns, σ_1 = 1500 barns, and σ_2 = 100 barns. The non-uniformity of the flux distribution across the rod has been allowed for. The neutron spectrum has been assumed to remain constant during the irradiation, and corrections to the values of σ_{c9} and σ_{c1} then made, following Appendix II(ii), to take into account the complicated behaviour of neutron capture in Pu^{240}. The final values, in barns, are given in Table 5.5.3. They are "average" values over the rod area and over the duration of the irradiation: their significance is discussed in the Appendix. Some comments on the values follow the table.

Table 5.5.3

Sample	P	G
σ_{c9}	431±8	427±3
σ_0	963±45	732±12
σ_{c1}	--	440±~30

$\underline{\sigma_{c9}}$: The errors given in Table 5.5.3 are those arising from uncertainties in the mass spectrometer measurements of the plutonium isotopic composition and the U^{235} depletion. There are other small uncertainties. An increase of 100 barns in the value assumed for σ_9 will decrease the calculated value of σ_{c9} by ~0.7 percent in G and by ~0.25 percent in P. An increase of 100 barns in the value assumed for σ_1 will increase σ_{c9} by ~0.25 percent in G and by a negligible amount in P. The correction for the non-constancy of σ_0 is 0.2 percent in G and is negligible in P. Uncertainties in the neutron flux distribution are not expected to introduce errors of more than 0.2 percent.

Before the data of P and G are compared, it should be pointed out that P, which was near the cooling water exit, was about 12° C hotter than G. The corresponding increase in σ_{c9} is expected to be 5 barns (Westcott, TNCC(CAN)-1), and the corrected difference between P and G is therefore only 1±10 barns.

An earlier value of 395±18 barns was calculated from the mass spectrometric analyses of a large number of plutonium samples obtained from different rods with irradiations between 800 and 3000 MWD/T. (See PM-320, which gives σ_{c9} = 370 barns based on $\sigma_f(U^{235})$ = 549 barns and E_f = 198 Mev/fission). In this study the neutron flux was calculated from the pile power, and part of the discrepancy (8±4 percent) between this estimate and the mean value of 427 barns from Table 5.5.3 may be due to an error in the assumed relation between flux and power. If E_f (200±6 Mev) were increased by three percent, the discrepancy would be reduced to 5±4 percent. The value of the initial plutonium production rate calculated from the measured conversion factor (Table 5.5.2) would be reduced to 0.88±0.01 gm/MWD, which is still in satisfactory agreement with the value 0.90±0.02 due to Barss.

Westcott (TNCC(CAN)-1) has calculated from neutron spectrometer data the effective values of σ_{c9} for maxwellian distributions at different temperatures. He has also estimated the contribution of the epithermal component of the neutron spectrum in an NRX rod (NDC-11). However, the quite important effect of the hardening of the neutron spectrum towards the centre of the rod is still being studied, and no final estimate of the expected value of σ_{c9} in a pile rod is available. Preliminary estimates give a value of about 400 barns for the average value across the rod.

$\underline{\sigma_0}$: It will be noted that the apparent value of σ_0 is some 30 percent greater in P than in G. The apparent decrease of this cross section with increasing irradiation has been observed previously (PM-320) and tentatively ascribed to self-shielding - a hypothesis apparently borne out by the radial distribution measurements. No quantitative interpretation of the data has yet been attempted.

$\underline{\sigma_{cl}}$: A calculation of σ_{cl} made on the assumption that σ_0 remains constant during the irradiation with the value given in Table 5.5.3 ignores the fact that the Pu^{241} is initially being produced at a higher rate and therefore underestimates the irradiation it has received. Consequently, such a calculation gives too high a value for σ_{cl}. A semi-quantitative estimate of this effect has been made in Appendix II: in the case of G, the overestimate is about five percent. It is not easy to assess the accuracy of this correction, and since the mass spectrometer analysis of Pu^{242} is uncertain to about ±5 percent, no complete investigation has been made.

F. The Radial Distribution of the Higher Isotopes of Plutonium

The detailed interpretation of the cross sections obtained in Section E requires a knowledge of the neutron spectrum as a function of depth in the rod, and of how this changes with irradiation. This knowledge is available, in principle at least, from a study of the radial variation of these cross sections in discs of different irradiation levels.

The value of the integrated flux for each sample was calculated from the A.N.L. flux distribution, corrected for the gradient across the rod (see Section B), and normalized to an absolute value by comparison with G (for H(A) and H(B)), with P (for Q(A)), and for O by assuming that the value of σ_{c9} at the surface of the rod was the same as in H. The radial direction of O is believed to be "B" on the evidence of the behaviour of σ_{c9} with depth.

The data from Q(B) have been excluded because of suspected contamination. Those from F and M have been omitted since the radial direction is unknown, only a few samples between 150 and 300 mil depth were analyzed, and in any case the irradiation levels were too close to H for there to be any useful increase in information.

The calculated cross-section values correspond to the appropriately weighted average, over the duration of the irradiation, of the neutron spectrum at each point. Their significance is discussed more fully in the Appendix. The results are shown in Fig. 5.5.4. The data from H(B), H(A), and O(B) show a smooth increase in the effective value of σ_{c9} towards the centre of the rod with a suggestion that this increase becomes less pronounced with increasing irradiation. Such behaviour is expected as the result of the thermal part of the neutron spectrum being hardened by absorption in the outer layers of the rod and the epithermal part having a flatter distribution across the rod. The latter effect is

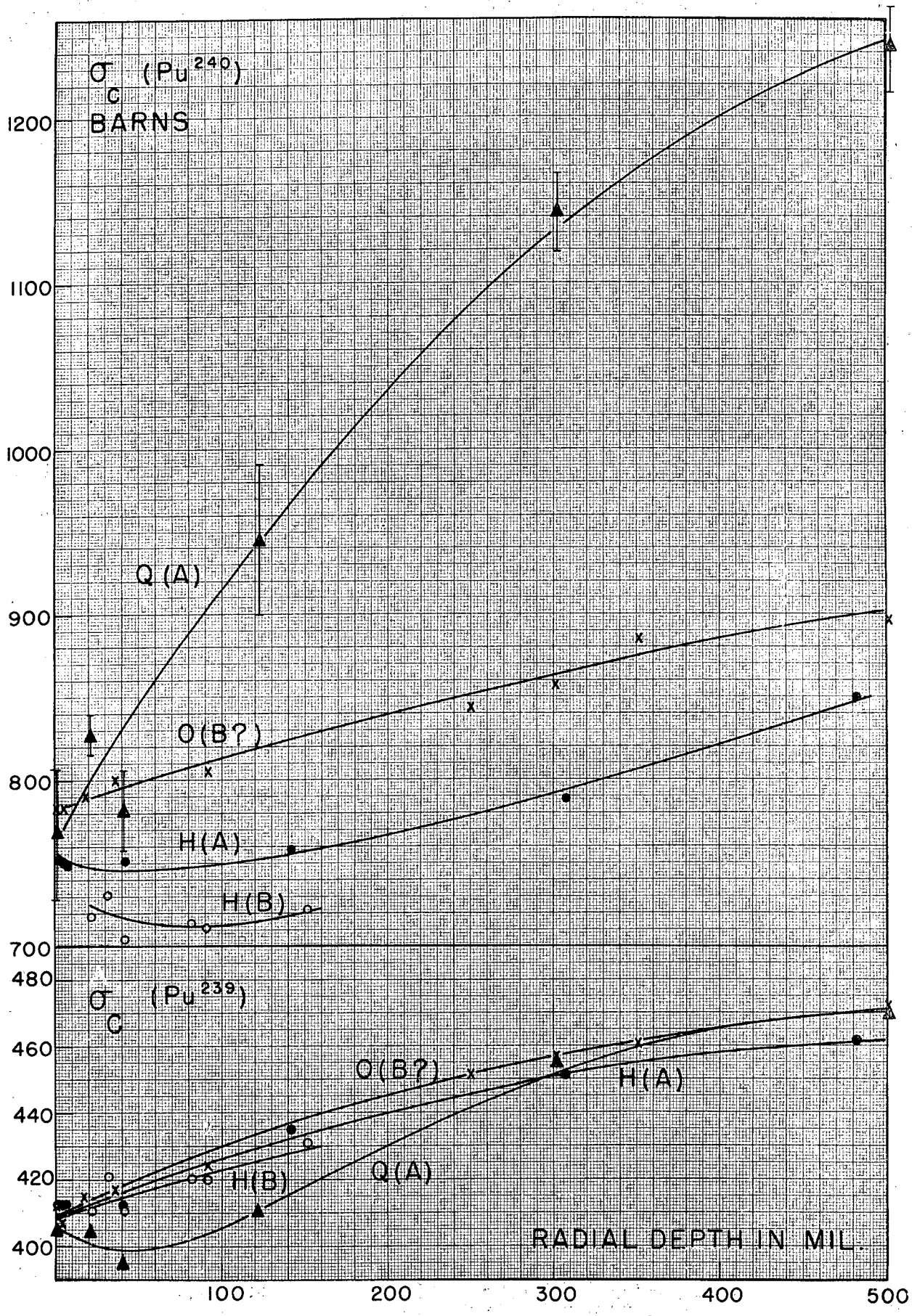

Fig. 5.5.4. The effective capture cross sections of Pu^{239} and Pu^{240} as functions of radial depth in Q(A), O, H(A), and H(B). The mass spectrometer errors are shown for $\sigma_c(240)$ in Q(A). These errors are less than one percent for all $\sigma_c(239)$ points and, for $\sigma_c(240)$ points, are about one percent in H(A) and H(B) and one to two percent in O.

expected to decrease as the Pu^{239} concentration increases and the absorption of the 0.3 ev resonance neutrons becomes more important. No quantitative interpretation of this self-shielding effect has, however, been attempted.

The results from Q(A) appear to be anomalous* and suggest a dip below the expected (A.N.L.) flux distribution in the region of 100 mil depth, as do the Cs^{137} and Pu/U data.

It may be observed that, if the mean value of the integrated flux across Q(A) is correct, no distribution can give the expected behaviour of σ_{c9}, that is, higher in Q(A) than in O at all points. Since Q was adjacent to P, for which the irradiation is accurately known, the mean value for Q(A) is expected to be too large only if the gradient across the rod has been underestimated: however the radial gamma-ray scan data, which indicate that the gradient is the same for Q as for H, are approximately confirmed by the Pu/U measurements in Q(A) and Q(B).

Fig. 5.5.4 also shows the apparent change with radius and irradiation of σ_0, the capture cross section of Pu^{240}. The important contribution from epithermal neutrons is shown by the pronounced rise towards the centre of the rod, an effect

---

* The fresh-rod Bessel-function distribution would give the following values for σ_{c9}:

Depth (mil)	1	21	41	122	302	502
Cross section (barns)	426	416	402	406	447	477

that is, a more pronounced anomaly of the same type.

that decreases rapidly as the irradiation increases because of self shielding. A quantitative treatment of this effect is beyond the scope of the present analysis, and, since it is not known to what extent the data of Q(A) are influenced by self shielding, it does not appear useful to attempt to derive a value for the resonance integral from the expected radial dependence of neutron spectrum in a fresh rod. In any case, the flux distribution across Q(A) is not well established.

The distribution of Pu^{242} has been measured in H and O, but the data are rather inaccurate. At the surface of the rod the apparent value of σ_{c1} is 435±15 barns, and there is some suggestion of an increase (perhaps 10 or 20 percent) towards the centre. An increase of about ɾ ven percent is expected to result from the change in the rate of Pu^{241} production during the irradiation (see Appendix II(ii)): the surface value would not be much affected since the apparent value of σ_0 at the rod surface remains fairly constant with increasing irradiation.

G. Summary

Data from the Complete Discs P and G

Accurate values of the integrated flux averaged across these discs have been obtained from careful measurements of the U^{235} depletion. The results, 0.661 n's/kb for G and 0.237 n's/kb for P, are not in agreement with predictions from pile-irradiation data.

Measurements of the plutonium produced give a value of 0.76±0.01 for the initial conversion factor and 0.91±0.01 gm/MWD for the initial production rate. These values imply that 27 percent of the plutonium is produced by resonance capture.

In both P and G, σ_{c9} = 427±3 barns, a value significantly higher than an earlier estimate (395 barns) based on pile irradiation data. The apparent decrease of σ_0 with increasing irradiation noted previously is again evident. The data of G give σ_{c1} = 440±~30 barns.

Data on Radial Distributions

U^{235} depletion measurements by A.N.L. across disc R (0.611 n's/kb) give a flux distribution slightly different from the fresh-rod Bessel-function distribution due to Hone. No useful information is obtained from the Cs^{137} data, and it has been necessary to assume that this A.N.L. distribution applies to all rod sections, although the radial distributions of both Pu^{239} and Pu^{240} suggest that this is not a good assumption.

The distribution of Pu^{239} indicates that about 2.5 percent of the total plutonium is formed as a thin skin on the rod surface.

The radial variation of σ_{c9} is not unexpected, but a quantitative interpretation would require more reliable flux data. σ_0 shows an increase towards the centre of the rod that is rapidly reduced by self shielding as the irradiation increases. The measurements of Pu^{242} are not very accurate, and the radial variation of σ_{c1} is not well defined.

APPENDIX

The Calculation of σ_{c9} and the Significance of the "Average" Values Obtained

SUMMARY

I. Small Sample - Constant Neutron Spectrum

The irradiation equations are given, and the dependence of the calculated value of σ_{c9} on the values assumed for other cross sections is tabulated.

II. Small Sample - Changing Neutron Spectrum

The neglect of changes - measured or estimated - in other cross sections introduces very small errors in the calculation of σ_{c9}.

The rather small changes of σ_{c9} itself can be interpreted accurately enough by the simple short-irradiation-approximation formulae. For example, if σ_{c9} increases linearly with the irradiation x from $\sigma(0)$ to $\sigma(x)$, the calculated value $\overline{\sigma}_{c9} = \sigma(0) + \frac{2}{3}(\sigma(x)-\sigma(0))$ with high accuracy for values of x in the range of interest.

III. Complete Disc - Constant Neutron Spectrum

The results of Section E were calculated on the assumption that all cross sections were independent of radius. The effects of the radial dependence of cross sections other than σ_{c9} itself are small. The significance of the average value of σ_{c9} is

discussed. For example, if σ_{c9} decreases parabolically with radius from σ at the centre to 0.9σ at the surface of the rod, the calculated value $\overline{\sigma}_{c9} = A\sigma$ where, for an NRX rod with $G_0 = 1.24$, $A = 0.94215$ at $\overline{x} = 0$ and 0.94461 at $\overline{x} = 0.9$ neutrons/kilobarn. The hypothetical case of a rod across which x is constant gives $A = 0.95$ at $x = 0$ and 0.94968 at $x = 0.9$.

IV. Complete Disc - Changing Neutron Spectrum

This case can be treated adequately by simple extensions of the results of II and III.

I. Small Sample - Constant Neutron Spectrum

If σ_8, σ_9, σ_0, σ_1, and σ_2 are the total absorption cross sections in kilobarns of U^{238}, Pu^{239}, Pu^{240}, Pu^{241}, and Pu^{242} and σ_{c9}, σ_{c1} are the capture cross sections of Pu^{239} and Pu^{241}, all of which remain constant during the irradiation, then after an irradiation of x neutrons/kilobarn (the same for all points in the sample), the concentration of each nuclide as an atom-fraction of the original U^{238} present, U, is:

$$U^{238}/U = \exp(-\sigma_8 x);$$

$$Pu^{239}/U = \sigma_8\left\{\frac{\exp(-\sigma_8 x)}{(\sigma_9-\sigma_8)} + \frac{\exp(-\sigma_9 x)}{(\sigma_8-\sigma_9)}\right\};$$

$$Pu^{240}/U = \sigma_8\,\sigma_{c9}\left\{\frac{\exp(-\sigma_8 x)}{(\sigma_9-\sigma_8)(\sigma_0-\sigma_8)} + \frac{\exp(-\sigma_9 x)}{(\sigma_8-\sigma_9)(\sigma_0-\sigma_9)} + \frac{\exp(-\sigma_0 x)}{(\sigma_8-\sigma_0)(\sigma_9-\sigma_0)}\right\};$$

$$Pu^{241}/U = \sigma_8\,\sigma_{c9}\,\sigma_0\left\{\frac{\exp(-\sigma_8 x)}{(\sigma_9-\sigma_8)(\sigma_0-\sigma_8)(\sigma_1'-\sigma_8)} + \frac{\exp(-\sigma_9 x)}{(\sigma_8-\sigma_9)(\sigma_0-\sigma_9)(\sigma_1'-\sigma_9)} + \frac{\exp(-\sigma_0 x)}{(\sigma_8-\sigma_0)(\sigma_9-\sigma_0)(\sigma_1'-\sigma_0)} + \frac{\exp(-\sigma_1' x)}{(\sigma_8-\sigma_1')(\sigma_9-\sigma_1')(\sigma_0-\sigma_1')}\right\}.$$

σ_1' includes the disappearance of Pu^{241} by beta decay. If the neutron flux, dx/dt, is constant during the irradiation, $\sigma_1' = \sigma_1 + \lambda t/x$.

The neglect of the finite lifetime of Np^{239} introduces only a small error in the quite long irradiation of rod 683 and has been neglected throughout.

These expressions may be expanded as series, which are more useful when x is small or in cases where x is different in

different parts of the sample. The series expansions are:

$$Pu^{239}/U = \sigma_8 x[1-\sigma^1(8,9)x/2!+\sigma^2(8,9)x^2/3!- \ldots\ldots];$$

$$Pu^{240}/U = \sigma_8\sigma_{c9}x^2[1/2!-\sigma^1(8,9,0)x/3!+\sigma^2(8,9,0)x^2/4!- \ldots\ldots];$$

$$Pu^{241}/U = \sigma_8\sigma_{c9}\sigma_0x^3[1/3!-\sigma^1(8,9,0,1)x/4!+\sigma^2(8.9,0,1)x^2/5!- \ldots\ldots];$$

$$Pu^{242}/U = \sigma_8\sigma_{c9}\sigma_0\sigma_{c1}x^4[1/4!-\sigma^1(8,9,0,1,2)x/5!+\sigma^2(8.9,0,1,2)x^2/6!- \ldots\ldots],$$

where $\sigma^n(8,9,0,1 \ldots)$ is the sum of all the products of degree n that can be formed from $\sigma_8, \sigma_9, \sigma_0, \sigma_1' \ldots$. For example, $\sigma^2(8,9) = \sigma_8^2 + \sigma_8\sigma_9 + \sigma_9^2$. They are readily formed by observing that, for example, $\sigma^n(8,9,0) = \sigma^n(8,9) + \sigma_0\sigma^{n-1}(8,9,0)$.

The second and higher terms of the infinite-series parts of these expressions will be generally referred to as the "destruction terms".

From the experimentally measured isotopic composition of the plutonium, it is possible to calculate $\sigma_{c9}\sigma_0$ and σ_{c1} if x, σ_8, σ_9, σ_1, and σ_2 are known. As an aid in the successive-approximation calculations, it is useful to calculate (from the original exponential expressions rather than from the series for the range of x required here) the quantities L, M, and N, defined by

$$\sigma_{c9}x/L = (Pu^{240}/Pu^{239}),$$

$$(\sigma_0/\sigma_{c9})/M = (Pu^{241}/Pu^{240})/(Pu^{240}/Pu^{239}),$$

$$(\sigma_{c1}/\sigma_0)/N = (Pu^{242}/Pu^{241})/(Pu^{241}/Pu^{240}),$$

for x at intervals of 0.1 n's/kb and for two or more values of

σ_0 200 barns apart. In the range of x involved here (0 to 0.9 n's/kb), L, M, and N change rather slowly and very smoothly with x and σ_0 (and σ_9, σ_1, and σ_2), and it is possible to interpolate between the calculated values with an accuracy of about 0.1 percent.

It may be seen from the series-expansion forms of the irradiation equations that, for short irradiations, the beta decay of Pu^{241} during the irradiation may be taken into account quite accurately by increasing the observed value of Pu^{241}/Pu^{240} by $\lambda t/4$ and decreasing that of Pu^{242}/Pu^{241} by $\lambda t/20$. This procedure is more convenient than that of increasing σ_1 by $\lambda t/x$, and for the present work, where $\lambda t \doteqdot 0.136$, it introduces at worst errors in the determinations of σ_{c9} and σ_0 of about 0.06 percent and 0.3 percent respectively. This is not considered important in view of the fact that, since the flux was not constant during the irradiation, the effective value of λt is uncertain by about ±10 percent.

In the irradiation range of interest, the value calculated for σ_{c9} (which is the only cross section that can be determined with both accuracy and significance) does not depend very seriously on the values assumed for σ_8, σ_9, and σ_1. For example, in the sample from H(A) at 1 mil depth, where x = 0.835 n's/kb, the dependence is summarized in the table:

For a 10 percent increase in	σ_8	σ_9	σ_1
The percentage increase in the calculated value of σ_{c9} is	$-5.5\ 10^{-3}$	-1.4_5	$+0.5_5$

Very approximately, the effect on σ_{c9} of a change in σ_8 or σ_9 is proportional to x and that of one in σ_1 to x^2.

II. Small Sample - Changing Neutron Spectrum

Fig. 5.5.4 shows that at a given point in the rod, the calculated value of σ_{c9} changes with irradiation, presumably as a result of the changing composition of the rod affecting the neutron spectrum. It is expected that the other cross sections are also affected, and indeed, near the centre of the rod, where self-shielding effects will be most important, the change in σ_0 with irradiation is very serious. The data shown in Fig. 5.5.4 were calculated on the assumption that all cross sections remained constant during the irradiation. The interpretation of these "average" $\bar{\sigma}_{c9}$ values will now be discussed.

In the over-simplified case where all other cross sections remain constant, where the irradiation is small enough for the destruction terms to be ignored, and where σ_{c9} increases linearly with irradiation x such that $\sigma_{c9} = \sigma_{c9}(0)(1+\alpha x)$, then

$$Pu^{239}/U^{238} = \sigma_8 x,$$

$$Pu^{240}/U^{238} = \sigma_8 \sigma_{c9}(0)[x^2/2 + \alpha x^3/3].$$

$\bar{\sigma}_{c9}$ is calculated from the constant-cross-section relation $Pu^{240}/Pu^{239} = \bar{\sigma}_{c9} x/2$,

whence $\bar{\sigma}_{c9} = \sigma_{c9}(0)(1 + 2\alpha x/3)$;

therefore $\sigma_{c9} = \sigma_{c9}(0) + (3/2)(\bar{\sigma}_{c9} - \sigma_{c9}(0))$ is the value at the end of the irradiation.

Given sufficient experimental data, a more complicated irradiation dependence could be evaluated by successive approximations.

The present section deals with the complications that are introduced by the variation of other cross sections and by the necessity of including the destruction terms in the analysis. The effects are sufficiently small to be investigated separately; that is, when the effect of the variation of the cross section(s) of one particular nuclide is being studied, the cross sections of all others are assumed to remain constant.

It is more convenient to discuss the derivation of σ_{c9} from the ratio R = (Pu^{240} left + Pu^{240} destroyed)/(Pu^{239} left), rather than from (Pu^{240}/Pu^{239}). The relation between σ_{c9} and (Pu^{240}/Pu^{239}) involves directly, as well as σ_8 and σ_9, the value of σ_0, which must itself be deduced from the measured Pu^{241} content. This requires a knowledge of σ_1 which, strictly, should be the sum of σ_{c1} (obtained from the Pu^{242} content and a knowledge - fortunately not crucial - of σ_2) and a value of σ_{f1} obtained from some other source and suitably corrected for the neutron spectrum involved. On the other hand, in the derivation of σ_{c9} from R, only σ_8 and σ_9 appear explicitly: in fact, for constant σ_8, σ_9, and σ_{c9}, $R = (\sigma_{c9}/\sigma_9)\left\{[(\sigma_9-\sigma_8)(1-\exp(-\sigma_8 x))/\sigma_8(\exp(-\sigma_8 x)-\exp(-\sigma_9 x))] - 1\right\}$.

It must be realized, however, that the calculation of R from the mass spectrometer data does involve σ_1, σ_{c1}, and σ_2: in fact, it will be seen that in practice, because of the lack

of reliable cross-section data from other sources and the limited accuracy of the Pu^{242} measurement, the two methods turn out to be exactly equivalent. Nevertheless, the effects on the value derived for σ_{c9} of variations in these higher cross sections are more easily evaluated by a consideration of their effects on the calculation of R rather than by a more direct attempt to modify the equations of Appendix I.

There would be no difficulty in calculating R from the mass spectrometer data if σ_1 and σ_{c1} were known accuracely from other sources,* and if the Pu^{242} content had been measured accurately. A knowledge of σ_2 is also required, but in practice a rough estimate is sufficient. The calculation of R would then proceed in the following way: first, an estimate of the Pu^{242} destroyed is required, which is obtained accurately enough from the short irradiation formula $(Pu^{242}\text{ destroyed})/(Pu^{242}) = (5/6)(\sigma_2/\sigma_{c1})(Pu^{242}/Pu^{241})$. This is then added to the measured Pu^{242} and then multiplied by $[(\sigma_1 + \lambda t/x)/\sigma_{c1}]$ to give the total Pu^{241} destroyed (and lost by beta decay), which is then added to the measured Pu^{241} to give the total Pu^{240} destroyed. R follows immediately, and σ_{c9} may then be calculated if σ_8, σ_9, and x are known. It will be noted that R is in no way affected by any peculiarities in the behaviour of σ_0 during the irradiation.

---

* Since $\lambda t/x \ll \sigma_1$, an accurate value of (σ_1/σ_{c1}) and a rough value of σ_1 would suffice.

Now σ_1 is not known accurately for the spectrum concerned (and may vary): this is a fundamental difficulty and introduces a basic uncertainty into any analysis of the results. A difficulty peculiar to the "R method" of calculating σ_{c9} is that σ_{c1} is not known - and, even if an accurate value were available, it would be inadvisable to use it because the Pu^{242} content is not known accurately. It is better to use the value of σ_{c1} calculated from the constant - cross-section equations of Appendix I so that the effect of the experimental error of the Pu^{242} determination is minimized (or, in fact, completely eliminated if the result is quoted as corresponding to a definite value of the total cross section σ_1). This calculation of R gives a value of σ_{c9} that is, necessarily, identical with that obtained from the analysis of Appendix I.

The error made in calculating R in this way is due to the incorrect estimation of the Pu^{241} destroyed, which arises from the fact that the value calculated for σ_{c1}, from the constant - cross-section equations, is in error. The effect of variations in σ_0, σ_1, and σ_{c1} during the irradiation on the calculation of the Pu^{241} destroyed, and hence on σ_{c9}, will now be considered. The very small effects of possible variations in σ_2 may be ignored.

(i) Variation in σ_1 and σ_{c1}

The value of R is not, in the cases of interest here, very sensitive to these cross sections, and an approximate calculation will be sufficient. The destruction terms will

be omitted (for the calculation of successive ratios of the higher isotopes, this is quite a close approximation because of the near-cancellation of the series), and only linear variations of σ_1 and σ_{c1} will be considered. The beta decay of Pu^{241} may be considered accurately enough as a separate correction and is omitted from the present discussion.

If $\sigma_{c1} = \sigma_{c1}(0)(1+\alpha_c x)$ and $\sigma_{f1} = \sigma_{f1}(0)(1+\alpha_f x)$, then, since $Pu^{241}/U = \sigma_8\sigma_{c9}\sigma_0 x^3/3!$,

$$Pu^{242}(+Pu^{243})/U = \sigma_8\sigma_{c9}\sigma_0\sigma_{c1}(0)x^4/4![1 + 4\alpha_c x/5]$$

$$\text{and } Pu^{241} \text{ F.P.'s}/U = \sigma_8\sigma_{c9}\sigma_0\sigma_{f1}(0)x^4/4![1 + 4\alpha_f x/5].$$

Therefore $r = (\text{total } Pu^{241} \text{ destroyed})/(Pu^{242} + Pu^{243}) =$

$$1 + \frac{\sigma_{f1}(0)(1 + 4\alpha_f x/5)}{\sigma_{c1}(0)(1 + 4\alpha_c x/5)} .$$

The constant - cross-section equations would give a value for σ_{c1},

$$\bar{\sigma}_{c1} = (4/x)(Pu^{242} + Pu^{243})/Pu^{241} = \sigma_{c1}(0)(1 + 4\alpha_c x/5),$$

so that $r = 1 + \sigma_{f1}(0)(1 + 4\alpha_f x/5)/\bar{\sigma}_{c1}$. That is, the value of σ_{f1} that should be used with $\bar{\sigma}_{c1}$ is $\sigma_{f1}(0)(1 + 4\alpha_f x/5)$.

A very rough estimate of the value of α_f may be made in the following way. Self-shielding effects in Pu^{241} will be negligible at present concentrations. If it is assumed that the resonance in Pu^{241} fission is about half as important (in its contribution to the effective cross section) as the resonance in Pu^{239} capture and that, being at the same energy, it is subject to the same reduction in epithermal flux, then, since the apparent change in $\bar{\sigma}_{c9}$ with irradiation is about

2/3 times the true change of σ_{c9}, it is expected that $\alpha_f x \doteq [(1/2)/(2/3)][\Delta\bar{\sigma}_{c9}/\bar{\sigma}_{c9}]$. At the centre of the rod a comparison between H and Q suggests $\Delta\bar{\sigma}_{c9}/\bar{\sigma}_{c9} \lesssim 0.1$, whence $4\alpha_f x/5 \lesssim 0.06$. Therefore, if no attempt were made to correct the value $\sigma_{f1}(0)$, an error of $\lesssim 4$ percent in r would be made. In the central H sample, the contribution to R from beyond Pu^{241} is only three percent. The error in R, and hence in σ_{c9}, would therefore be at most 0.1_2 percent.

The uncertainty in the appropriate value of $\sigma_{f1}(0)$ is, at present, more important, but this approximate analysis of the effect of variations is included in the hope that, with more accurate data, it may eventually be useful.

(ii) Variations in σ_0

As in (i), approximate equations may be used. It is assumed that a linear variation of σ_0 with irradiation is reasonably representative of the actual behaviour (which is certainly more complicated than this, but is not yet well defined).

It is easily shown that with $\sigma_0 = \sigma_0(0)(1-\alpha x)$,

$$Pu^{241}/Pu^{240} = \bar{\sigma}_0 x/3 = (\sigma_0(0)x/3)(1 - 3\alpha x/4)$$
$$\text{and } Pu^{242}/Pu^{241} = \bar{\sigma}_{c1} x/4 = (\sigma_{c1} x/4)(1 - 3\alpha x/20),$$

where $\bar{\sigma}_0$ and $\bar{\sigma}_{c1}$ are the values calculated from the constant-cross-section equations.

Therefore $\sigma_{c1} = \bar{\sigma}_{c1}/(1 + (\sigma_0(0)-\bar{\sigma}_0)/5\sigma_0(0))$.

Near the surface of the rod, $\sigma_0(0) \approx \bar{\sigma}_0$ (compare Q and H in Fig. 5.5.4), but near the centre, $\sigma_0(0)$ ($\gtrsim \bar{\sigma}_0$ for Q)

$\doteq$ 1300 barns, and $\bar{\sigma}_0$ for H $\doteq$ 850 barns. Therefore, in the centre of H, $\sigma_{c1} \doteq \bar{\sigma}_{c1}/(1 + 0.35/5) = 0.93\ \bar{\sigma}_{c1}$; and if σ_{c1} were used with a hypothetically correct value of σ_{f1}, the error in r, proportional to $(1 + \sigma_{f1}/\sigma_{c1})$, would be -5 percent. The resulting underestimate of σ_{c9} would therefore be (see (i) above) about 0.15 percent.

For heavier irradiations, σ_{c9} would be more dependent on r (almost as x^2), but the change in σ_0 is less marked in these samples. Although the analysis given here is very approximate, it is evident that the neglect of the variation of σ_0 leads to an underestimate of σ_{c9} by less than two barns in all cases.

(iii) Variation in σ_8

In the absence of reliable experimental data, it will be assumed that $\sigma_8 = \sigma_8(0)(1+\alpha x)$. The destruction of U^{238} may safely be ignored since its effect on σ_{c9} is small and will be nearly the same in the two cases to be compared, viz., $\alpha = 0$ and $\alpha \neq 0$ with $\alpha x < 1$ (see table in Appendix I).

It can then be shown that

$$R = \frac{\sigma_{c9}}{\sigma_9} \frac{(1 - \alpha/\sigma_9)(\sigma_9 x - [1-\exp(-\sigma_9 x)]) + \alpha\sigma_9 x^2/2!}{(1 - \alpha/\sigma_9)[1-\exp(-\sigma_9 x)] + \alpha x}$$

$$= \frac{\bar{\sigma}_{c9}}{\sigma_9} \frac{\sigma_9 x - [1-\exp(-\sigma_9 x)]}{[1-\exp(-\sigma_9 x)]},$$

where $\bar{\sigma}_{c9}$ is the value calculated from the constant - cross-section equations, that is, with $\alpha = 0$.

$$\text{Whence } \frac{\bar{\sigma}_{c9}}{\sigma_{c9}} = \frac{1 + [w/(w-1)]\, z^2/(2z-2[1-\exp(-z)])}{1 + [w/(w-1)]\, z/[1-\exp(-z)]},$$

where $w = \alpha/\sigma_9$ and $z = \sigma_9 x$.

For small z, $\bar{\sigma}_{c9}/\sigma_{c9} \rightarrow (1 + \alpha x/3)/(1 + \alpha x/2) \approx (1 - \alpha x/6)$.

It should also be noted that, independent of the value of z, the value of σ_8 calculated from the plutonium produced, $\bar{\sigma}_8$, is equal to $\sigma_8(0)(1 + \alpha x/2)$. Numerically, for $\bar{\sigma}_8 = 1.05\sigma_8(0)$, that is, $\alpha x = 0.1$, and for $\sigma_9 = 1300$ barns, $\bar{\sigma}_{c9}$ is less than σ_{c9} by 1.926 percent when $x = 0.5$ n's/kb, and by 2.257 percent when $x = 1.0$ n's/kb.

The experimental data on the change of σ_8 with irradiation have been discussed in Section D. At present, because of uncertainties in the neutron flux distribution and in the appropriate value of σ_9, it is not possible to rule out a change of up to five percent in $\bar{\sigma}_8$. It should be noted, however, that since about 75 percent of the plutonium is produced by thermal neutrons (Section D), a change of 10 percent in σ_8 (about five percent in $\bar{\sigma}_8$) would imply a change of nearly 50 percent in the ratio of resonance to thermal flux, which is much greater than that expected to result from the changes in neutron absorption properties of the rod produced by irradiation. A rather rough calculation suggests that in the centre of the rod this ratio will increase by about two percent between Q and H. The effect on the calculated value of σ_{c9} would be ~0.1 percent.

(iv) Variations of σ_{c9} and σ_9

It is now assumed that the effects of the variation of all other cross sections have been corrected for, and it remains to discuss the interpretation of $\bar{\sigma}_{c9}$, the value obtained from the constant - cross-section equations, when σ_{c9} and σ_9 themselves change with irradiation. Because of uncertainties in the flux distribution, no firm conclusions on the experimentally observed behaviour of $\bar{\sigma}_{c9}$ can yet be drawn, and the present discussion is limited to the case, which is expected to be realized approximately in practice, where σ_{c9} and σ_9 change linearly with irradiation.

Neglecting the destruction of U^{238} as in (iii), then for $\sigma_9 = \sigma_9(0)(1+\alpha x)$,

$$\frac{d}{dx}(Pu^{239}) + \sigma_9(0)(1+\alpha x)Pu^{239} = \sigma_8 U.$$

This may be solved in series form to give

$$\begin{aligned} P = Pu^{239}/U = \sigma_8 x[1 &- (1+b_1\alpha x)(\sigma_9(0)x)/2! \\ &+ (1+c_1\alpha x+c_2\alpha^2x^2)(\sigma_9(0)x)^2/3! \\ &- (1+d_1\alpha x+d_2\alpha^2x^2+d_3\alpha^3x^3)(\sigma_9(0)x)^3/3! \\ &+ \text{etc.}], \end{aligned}$$

where the coefficients of $\alpha^n x^n$ in the (finite) subsidiary series are given by

$3b_1 = 2$

$4c_1 = 3(1+b_1)$ $\quad 5c_2 = 3b_1$

$5d_1 = 4(1+c_1)$ $\quad 6d_2 = 4(c_1+c_2)$ $\quad 7d_3 = 4c_2$

$6e_1 = 5(1+d_1)$ $\quad 7e_2 = 5(d_1+d_2)$ $\quad 8e_3 = 5(d_2+d_3)$ $\quad 9e_4 = 5d_3$

$7f_1 = 6(1+e_1)$ $\quad 8f_2 = 6(e_1+e_2)$ $\quad 9f_e = 6(e_2+e_3)$ $\quad 10f_4 = 6(e_3+e_4)$

etc. $\qquad$ etc. $\qquad$ etc. $\qquad$ etc.

If, now, $\sigma_{c9} = \sigma_{c9}(0)(1+\gamma x)$,

then $Q = (Pu^{240}$ left + Pu^{240} destroyed$)/U = \sigma_{c9}(0)\int(1+\gamma x)P\,dx$

$= \sigma_8\sigma_{c9}(0)x^2\{(1/2 + \gamma x/3) - [(1/3 + \gamma x/4) + (1/4 + \gamma x/5)b_1\alpha x]\sigma_9(0)x/2!$

$+ [(1/4 + \gamma x/5) + (1/5 + \gamma x/6)c_1\alpha x + (1/6 + \gamma x/7)c_2\alpha^2x^2](\sigma_9(0)x)^2/3!$

$-$ etc.$\}$

It may be noted that for $\gamma = \alpha$, $Q = (\sigma_{c9}(0)/\sigma_9(0))(\sigma_8 x - P)$.

If the first two terms only of the series for P and Q are retained, then

$$R = Q/P \doteq \sigma_{c9}(0)(1 + 2\gamma x/3)(x/2)[1+\sigma_9(0)(1 + \alpha x - \gamma x/6)x/6].$$

This suggests that, for small x, the constant - cross-section analysis will give $\bar{\sigma}_{c9} \doteq \sigma_{c9}(0)(1 + 2\gamma x/3)$ if a value for the total cross section $\bar{\sigma}_9 = \sigma_9(0)(1 + \alpha x - \gamma x/6)$ is used.

In order to see how close this approximation is for finite x, two cases have been evaluated numerically for

$x = 0.661$ n's/kb $\quad \sigma_{c9}(0) = 425$ barns $\quad \sigma_9(0) = 1300$ barns

Case (i) $\alpha x = \gamma x = 0.1$ $\quad R = 0.1728850$

whence, with $\bar{\sigma}_9 = 1300(1 + 0.1 - 0.1/6) = 1408.333$ barns, the constant - cross-section analysis gives

$$\bar{\sigma}_{c9} = 453.705 \text{ barns} = (1 + 2\gamma x/3)425.348 \text{ barns}.$$

Case (ii) $\alpha x = 0.1$ $\quad \gamma x = 0.15$ $\quad R = 0.1781039$

whence, with $\bar{\sigma}_9 = 1300(1 + 0.1 - 0.15/6) = 1397.5$ barns,

$$\bar{\sigma}_{c9} = 467.865 \text{ barns} = (1 + 2\gamma x/3)425.331 \text{ barns}.$$

It is evident that, for the irradiation levels of interest here, first approximation methods are adequate for the study of the variation of σ_{c9} with irradiation, since they introduce errors that are smaller than those due to uncertainties in the appropriate values of σ_9 and σ_1.

III. Complete Disc - Constant Neutron Spectrum

In this section the significance of the average values of σ_{c9} derived from the data on the complete discs P and G will be discussed assuming that the neutron spectrum remains constant at each point in the disc. This necessarily implies that the flux distribution remains constant during the irradiation.

It will be assumed that σ_8 has the same value at each point. This neglect of the plutonium skin introduces a very small error, which has actually been allowed for in deriving the results of Section E, but which is not of interest in the present discussion. The destruction of U^{238} may again be ignored.

If y is the radius of the ring having an irradiation x (with y = 1 at the rod surface), then

$$R = \int(240 \text{ left} + 240 \text{ destroyed})dV / \int(Pu^{239} \text{ left})dV$$

$$= \frac{\int_0^1 [\sigma_{c9}x^2/2! - \sigma_{c9}\sigma_9 x^3/3! + \sigma_{c9}\sigma_9^2 x^4/4! - \ldots\ldots]2\pi y\, dy}{\int_0^1 [x - \sigma_9 x^2/2! + \sigma_9^2 x^3/3! - \ldots\ldots]2\pi y\, dy}.$$

As a reasonable approximation to the actual flux distribution, it is assumed that $x = x(c)(1+ky^2)$ where x(c) is the irradiation level on the rod axis. It is evident that the mean irradiation of the disc $\bar{x} = \int_0^1 x\, 2\pi y\, dy / \int_0^1 2\pi y\, dy = x(c)(1+k/2)$.

The observed variations of σ_{c9} and σ_9 are adequately represented by the expressions

$$\sigma_{c9} = \sigma_{c9}(c)(1-ay^2),$$
$$\sigma_9 = \sigma_9(c)(1-by^2).$$

An exact solution has been attempted only for a = b.

Writing $\sigma_{c9}(c) = \sigma$ and $\sigma_9(c) = S$,

$$R = \frac{N_2R_2\sigma(\bar{x})^2/2! - N_3R_3\sigma S(\bar{x})^2/3! + N_4R_4\sigma S^2(\bar{x})^3/4! - \ldots\ldots}{N_1R_1\bar{x} - N_2R_2S(\bar{x})^2/3! + N_3R_3S^2(\bar{x})^3/3! - \ldots\ldots}$$

where $R_n = [(1+k)^{n+1} - 1]/[(n+1)k(1 + k/2)^n]$

and $N_n = 1$ for $a(= b) = 0$;

and for $a(= b) \neq 0$,

$$N_n = 1 - \left\{\frac{2(n+1)k}{(1+k)^{n+1} - 1}\right\}\left\{(n-1)a\left(\frac{1}{4} + \frac{nk}{6} + \frac{n(n-1)}{2!}\frac{k^2}{8} + \frac{n(n-1)(n-2)}{3!}\frac{k^3}{10} + \ldots\right)\right.$$
$$- \frac{(n-1)(n-2)a^2}{2!}\left(\frac{1}{6} + \frac{nk}{8} + \frac{n(n-1)}{2!}\frac{k^2}{10} + \frac{n(n-1)(n-2)}{3!}\frac{k^3}{12} + \ldots\right)$$
$$\left. + \frac{(n-1)(n-2)(n-3)a^3}{3!}\left(\frac{1}{8} + \frac{nk}{10} + \frac{n(n-1)}{2!}\frac{k^2}{12} + \frac{n(n-1)(n-2)}{3!}\frac{k^3}{14} + \ldots\right)\right.$$
$$\left. - \text{etc.}\right\}.$$

It is evident that, for small $\bar{x}$, the value $\bar{\sigma}$ obtained for σ_{c9} on the assumption that it had the same value at all depths would be equal to $N_2\sigma$.

For k = 0.6316, which gives $G_0 = 1.24$ (the experimentally observed value), $N_2 = 0.9421505$ for a = 0.1 and 0.8843010 for a = 0.2, whereas for k = 0, $N_2 = 0.95$ for a = 0.1 and 0.90 for a = 0.2. It has been shown that this relationship between $\bar{\sigma}$ and σ is not appreciably altered by increasing irradiation. Values of R have been calculated with $\sigma(1-a)$ and $S(1-a)$, the

rod surface values of σ_{c9} and σ_9, equal to 425 and 1300 barns respectively, for $\bar{x}$ = 0.3, 0.6, and 0.9 n's/kb and a = 0.1 and 0.2. From these values of R, values of $\bar{\sigma}$ were then calculated from the series appropriate to the case of σ_{c9} and σ_9 independent of radius (that is, with all N_n set equal to unity and S replaced by $\bar{S}$). In this calculation it was assumed that $\bar{S} = \bar{\sigma}(1300/425)$, which necessitated successive approximation calculations: very similar results would have been obtained with $\bar{S} = N_2 S$, the zero-irradiation approximation. The table below shows the percentage by which $\bar{\sigma}$ differs from σN_2 (= $\bar{\sigma}$ at x = 0).

	k = 0			k = 0.6316		
$\bar{x}$	0.3	0.6	0.9	0.3	0.6	0.9
a = 0.1	-.012	-.023	-.034	+.094	+.181	+.261
a = 0.2	-.059	-.111	-.159	+.181	+.350	+.515

It is evident that the use of the zero-irradiation approximation will introduce errors that in all practical cases are less than that arising from the uncertainty in σ_9.

The case with b ≠ a has not been evaluated completely, but enough has been done to show that with b < a (which is the case of interest), the deviations for a given a will be smaller than for b = a.

It is reasonable to suppose that the irradiation dependence will also be unimportant in cases where the variation of cross section with radius is non-parabolic, providing it is not too violent.

The effects of radial variations of the higher cross sections (σ_0, σ_1, etc.) can be examined by integration of the approximate (zero x) irradiation formulae over the rod area in order to evaluate the error made in calculating the Pu^{241} destruction (compare Appendix II). The effects on σ_{c9} are negligible.

IV. Complete Disc with Changing Spectrum

It is evident from III that since $\overline{\sigma}/\sigma$ is not very sensitive to k, a reasonably small change in the neutron flux distribution across the disc will not in itself introduce a significant error.

However, the accompanying spectrum change will alter the value of σ_{c9} at any given point in the disc. Now it has been shown that $\overline{\sigma}$ is very close to the zero-irradiation average σN_2 for all irradiation levels of interest. Therefore, once the k weighting (that is, the factor N_2) has been taken into account, the system can be treated accurately enough as a small sample (Appendix II) in which the cross section changes with irradiation in the same way as the average cross section across the disc changes.